Light-meson light-cone distribution amplitudes from QCD sum rules and their applications: A mini-review

Xing-Gang Wu

In collaboration with

Tao Huang, Tao Zhong, Hai-Bing Fu, Hua-Yong Han, Wei Cheng, Yi Zhang, Dan-Dan Hu, Long Zeng, et al.

Department of Physics, Chongqing University

2026.11.06-11.09, USTC

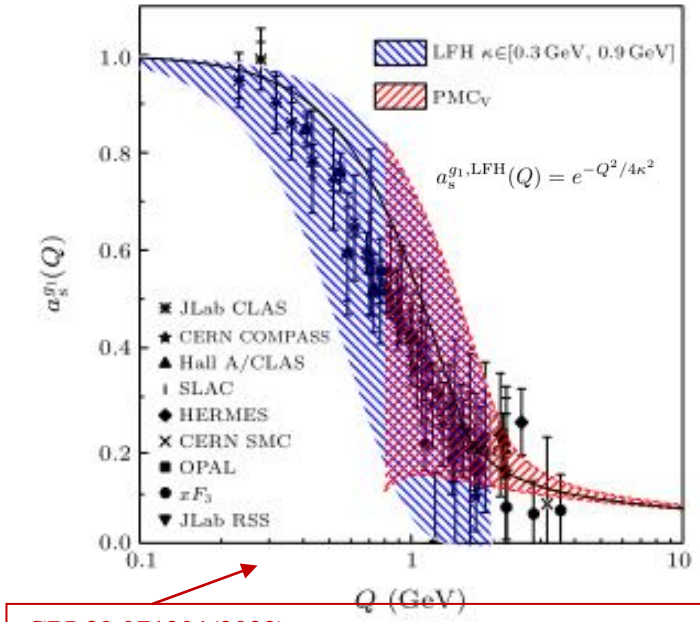
Starting from 2008

Contents

1. QCD sum rules (QCDSR)
2. Sum rules for the light-meson LCDAs (<ξ>-moments)
3. Applications of the light-meson LCDAs

   (Light-cone sum rules for heavy-to-light transitions)
4. Summary and Outlook

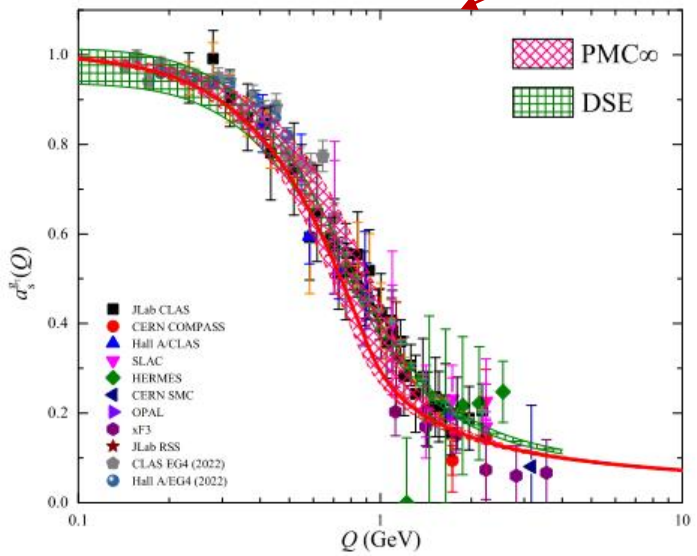
Methodology：QCDSR + and/or { Data, LQCD, Model }



CPL39,071201(2022)

Red band is uncertainty caused by UHO-terms and $\Delta\alpha_s(M_z)= \pm 0.0010$

PRD111,114003(2025)



The QCD Lagrangian

$$\mathcal{L}_{QCD} = -\frac{1}{4}G^a_{\mu\nu}G^{a\mu\nu} + \sum_q \bar{\psi}_q(i\not{D} - m_q)\psi_q$$

There exist bound-state effects driven by quark -gluon fluctuations in vacuum; **Perturbation** theory can only describe strong interactions in high-energy region; Typical **Non-perturbative ways**: QCD SR and LQCD

$$R_{hadr} \sim 1/\Lambda_{QCD}$$

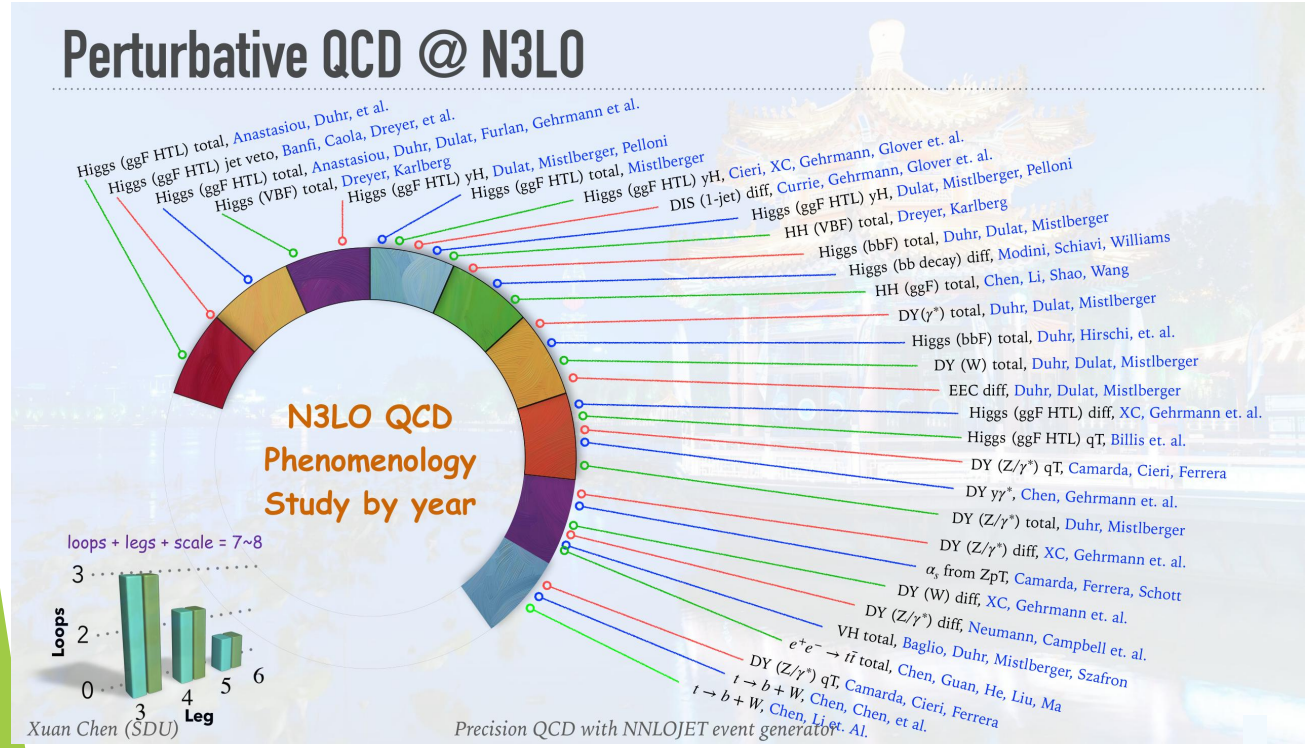
For hadron-related processes, the hadronic parts — which are affected by quark-confinement bound-state effects — must be treated with appropriate non-perturbative methods

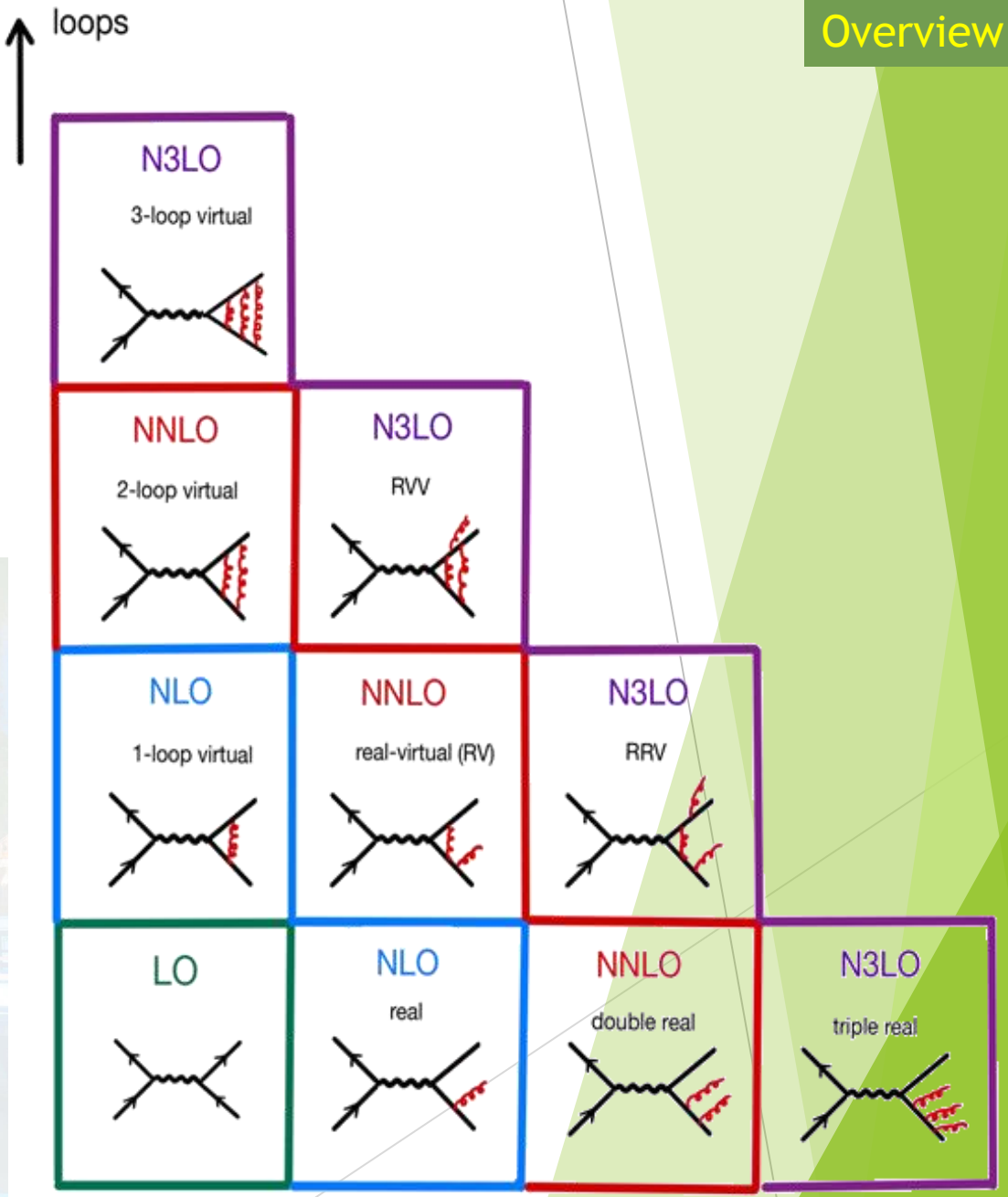
It is important to know the physical observables in whole scale region

微扰论大势已成

Perturbation theory is now firmly established

$$\sigma = \sum_{a,b} \int_0^1 \mathrm{d}x_a\, \mathrm{d}x_b\, f_{a/h_1}(x_a)\, f_{b/h_2}(x_b)\, \mathrm{d}\hat{\sigma}_{ab\to n} + \mathcal{O}\left(\frac{\Lambda_{\mathrm{QCD}}}{Q}\right)^p$$





微扰理论的优点、局限性及待解难题

The Merits, Limitations, and Open Problems of Perturbation Theory



Assumption/Merits

Coupling g < 1 ⇒ order-by-order computation gives reliable estimates, exemplifying human explanation and prediction (analytic at heart)



Limitations

Higher-order terms are capped by loop-computation ability;

Unknown-Higher Order terms

UHO⇒ unavoidable theory error

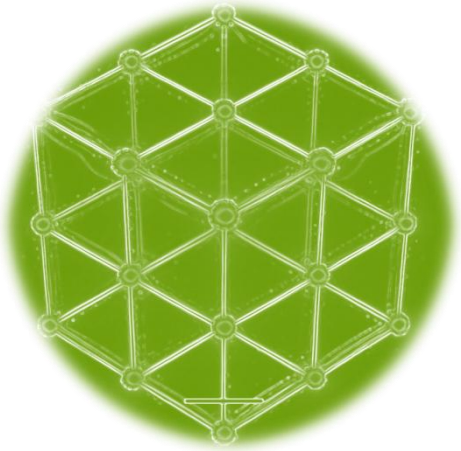


Challenges

For precise perturbative prediction, two challenges must be met:

- ***Obtain fixed-order RGI-results independent of any choices of renormalization scale and renormalization scheme ;***
- ***Reliably and precisely estimate the error from the UHO-terms***

格点QCD：基于第一性原理的非微扰数值基石
Lattice QCD: The First-Principles Non-Perturbative Cornerstone



Lattice QCD discretizes continuous spacetime onto a four-dimensional lattice, offering a **systematic first-principles approach** to deal with quark confinement in the low-energy regime. Using **Monte Carlo simulation**, it computes the strong interaction of quarks and gluons directly from the QCD Lagrangian — **The core tool for solving non-perturbative problems**

Key assumption: **Euclidean results continue back to Minkowski + the a→0 limit exists**

四个技术挑战 —— Four Technical Challenges

算力指数爆炸
01 · Explosive Compute
Fine spacing for cutoff; cost scales as volume to fourth power — a heavy load

有限体积矛盾
02 · Finite-Volume Dilemma
Fine spacing vs. large physical volume; boundary effects on long-range forces compete

系统误差叠加
03 · Accumulating Systematics
Renormalization, discretization, and chiral extrapolation all add uncertainty

高噪信噪比差
04 · Poor Signal-to-Noise
High-momentum signals are masked by noise, needing huge Monte Carlo sampling

QCD求和规则：连接微扰与非微扰的解析桥梁

QCD Sum Rules: Analytical Bridge between Perturbative and Non-Perturbative QCD

Correlator $\Pi(q^2)$ analytical in whole q^2-region

QCD sum rules represent hadrons not as constituent-quark bound states but as the quantum-number projection of **interpolating quark currents** at large virtuality. At large space-like $Q^2(>0;\ q^2 = -Q^2 < O)$, the correlator is computed perturbatively plus vacuum condensates (or light-cone distribution amplitudes); at time-like $q^2 < O$, it becomes a sum over physical hadronic states. Equating the two via dispersion relations yields predictive constraints on **hadron masses, decay constants, form factors and quark masses** — the leading analytical complement to lattice QCD.

非微扰QCD中占据一席之地 —— Its Place in the Non-Perturbative QCD Toolbox

解析性	模型无关性	普适真空凝聚态	广泛研究内容
01 Analytical	**02 Model-independent**	**03 Universal condensates**	**04 Wide reach**
Complementary to numerical LQCD; no discretization noise	No constituent wave function; quantum numbers from current	Extracted from one channel, reused across many others	Masses, f_V, form factors, baryons, HQET

主要局限：求和规则的精度边界

Where the Method Is Stretched: Four Principal Uncertainties

算符展开截断有效性
01. Effectiveness of the OPE truncation

The power series in $\Lambda_{\mathrm{QCD}}^2/Q^2$ is usually truncated at d=6 or d=8. Higher-dimensional condensates (d≥7) are poorly known and suppressed by Borel transformation. **At low M^2 the omitted contributions can be nonnegligible**, affecting effectiveness of OPE.

夸克强子对偶近似
02. Quark-hadron duality

Replacing spectral density above s_0 by the perturbative answer is a "semilocal" assumption, not a strict consequence of asymptotic freedom. In some channels (e.g. scalar / pseudo-scalar) **no Borel window exists** — "direct instantons" break the OPE.

凝聚项误差
03. Condensate uncertainties

Still with **large uncertainty**. The gluon condensate carries ±30% error; four-quark terms rely on factorization $\langle\bar{\psi}\Gamma\psi\bar{\psi}\Gamma\psi\rangle \sim \langle\bar{\psi}\psi\rangle^2$. These non-perturbative inputs set floor on predictive accuracy.

$$\langle\bar{q}q\rangle = \langle 0|\bar{\psi}_\alpha\psi_\beta|0\rangle = -\,\mathrm{Tr}[S_F(0)]$$

$$\langle\bar{q}q\rangle|_{2\ \mathrm{GeV}} = (-289.14^{+9.34}_{-4.47})^3\ \mathrm{MeV}^3,$$
$$\langle g_s\bar{q}\sigma TGq\rangle|_{2\ \mathrm{GeV}} = (-1.934^{+0.188}_{-0.103})\times 10^{-2}\ \mathrm{GeV}^5,$$
$$\langle g_s\bar{q}q\rangle^2|_{2\ \mathrm{GeV}} = (2.082^{+0.734}_{-0.697})\times 10^{-3}\ \mathrm{GeV}^6,$$
$$\langle g_s^2\bar{q}q\rangle^2|_{1\ \mathrm{GeV}} = (7.420^{+2.614}_{-2.483})\times 10^{-3}\ \mathrm{GeV}^6,$$
$$\langle\alpha_s G^2\rangle|_{1\ \mathrm{GeV}} = 0.038(11)\ \mathrm{GeV}^4,$$
$$\langle g_s^3 fG^3\rangle|_{1\ \mathrm{GeV}} \approx 0.045\ \mathrm{GeV}^6,$$

参数与模型依赖
04. Parameter & model dependence

Results depend on the choice of Borel mass M^2, continuum thre-shold s_0, and renormalization scale μ. Poles extracted from sum rules (e.g. in X(2370)-type analyses) can be **model-dependent** and not uniquely identify a physical state.

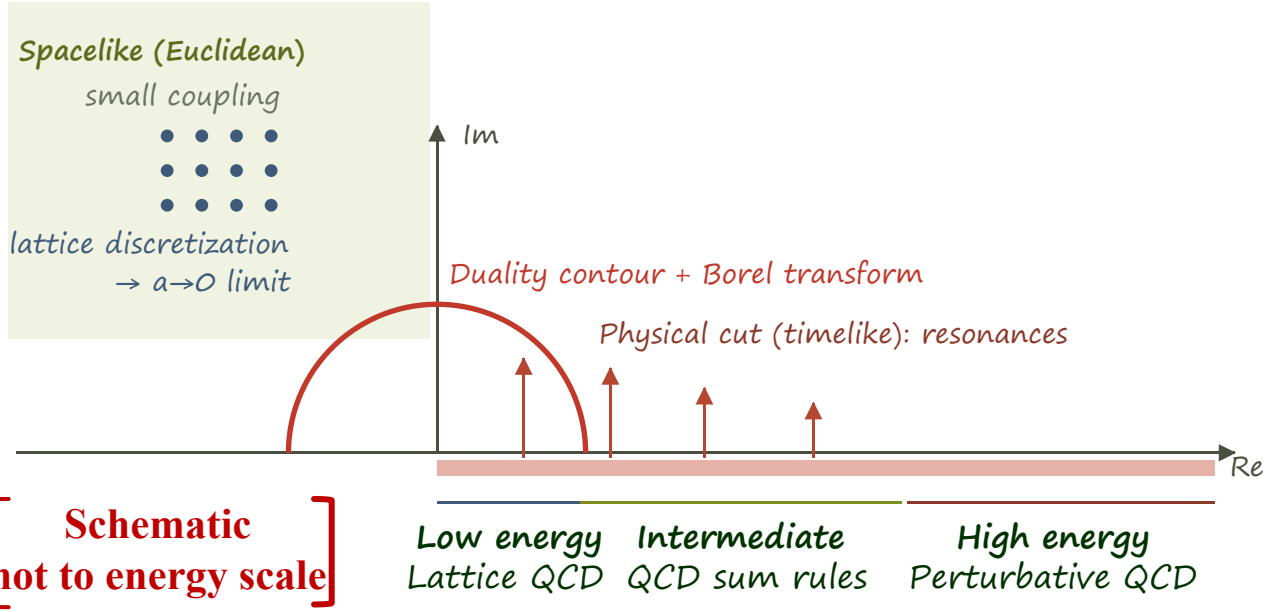
求和规则是一种可靠但近似的解析工具 —— 在*Borel*窗口存在区间内可与格点 *QCD* 相竞争，但物理过程相关且需给出恰当的误差估计

Bottom line: sum rules are a reliable but approximate analytical tool — competitive with the lattice QCD where the Borel window exists, but must be applied case by case with honest error estimates.

Three methods: 互补 (Complementary) + 连贯 (Coherent)

Complex momentum-transfer plane

Left: computable directly. Right: needs continuation and duality



Lattice QCD

Non-perturbative · first principles | window: low energy (small q^2)

Core assumption: discretization + a → 0 limit exist; Euclidean results need analytic continuation

Small parameter: $a\Lambda_{\mathrm{QCD}}$, $1/(L\Lambda_{\mathrm{QCD}})$ | errors assessed item by item

QCD Sum Rules

Perturbative + non-perturbative · the bridge | window: intermediate energy

Core assumption: quark–hadron duality in the Borel window + OPE truncation + vacuum saturation

Small parameter: $1/Q^2$ (Λ^2/Q^2) | errors hard to systematize

Perturbative QCD

Perturbative · hard process | window: high energy (large q^2)

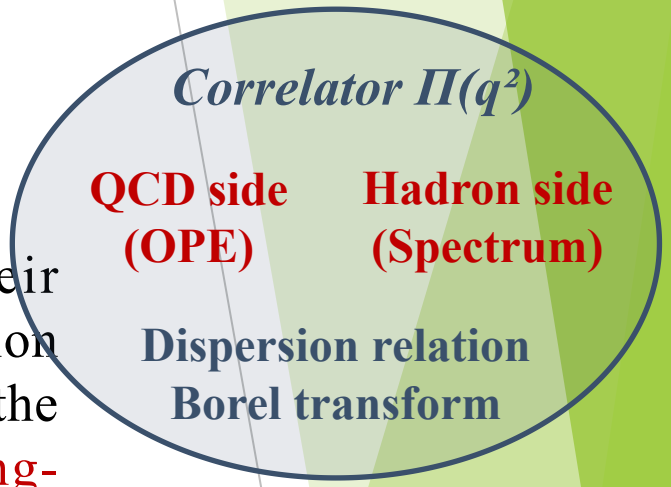
Core assumption: $\alpha_s \ll 1$ and factorization — IR input separable from hard coefficients

Small parameter: $\alpha_s(Q^2)$ | improvable order by order, renormalon-limited

In different energy regions, various methods each play to their own strengths and complement one another;
By combining these methods, a coherent description of the complete physical region can be obtained

1. The QCD sum rules

Basic idea of QCD sum rules



Within the QCD sum rule approach, hadrons are represented by their interpolating quark currents taken at large virtualities. The correlation function (**Collerator**) of these currents is introduced and treated in the framework of the operator product expansion (OPE), where the short-distance and the long-distance quark-gluon interactions are separated. The former are calculated using QCD perturbation theory, whereas the latter are parametrized in terms of universal vacuum condensates (SVZ sum rules) or light-cone distribution amplitudes (LCSR). The result of the QCD calculation is then matched, via dispersion relation, to a sum over hadronic states.

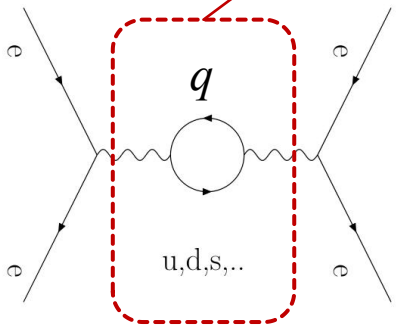
SVZ 方法试图从 QCD 第一原理出发，从小距离来逼近共振态物理。更确切地说，是在 QCD 标符级权展开的基础上，考虑了非微扰效应，引入非零的标符真空平均值，借助于色散关系以解决强子共振态的非微扰问题的。**How to do ?**

QCD求和规则的基础构建恰当关联函数
Basis for QCD SR — In the $q^2<0$ space-like region

Typical example:

电磁流守恒 $\partial_\mu j^\mu = 0$

$$\Pi_{\mu\nu}(q) = i\int d^4x\, e^{iq\cdot x}\langle 0|\, T\{j_\mu(x) j_\nu(0)\}\,|0\rangle = (q_\mu q_\nu - q^2 g_{\mu\nu})\Pi(q^2)$$



真空极化振幅-虚光子自能修正
(Vacuum polarization amplitude)

$\mathrm{Im}\,\Pi = 0$, $\Pi(q^2)$ 实而光滑

One-side: $Q^2 \equiv -q^2 \gg \Lambda^2_{QCD}$

Dominated within $|\vec{x}| \sim x_0 \sim 1/\sqrt{Q^2} \ll R_{hadr}$

Thus, calculable via OPE

$$\Pi(q^2) = \sum_d C_d(q^2)\langle 0|\, O_d\,|0\rangle$$

真空凝聚项按量纲排列，高维算符有Q^2-幂次压低

$C_0(q^2) = \Pi^{pert}(q^2),\ \langle 0|\, O_0\,|0\rangle \equiv 1$

PHYSICAL REVIEW D VOLUME 39, NUMBER 4 15 FEBRUARY 1989

Quantum chromodynamics in background fields

Tao Huang
Center of Theoretical Physics, Chinese Center of Advanced Science and Technology (World Laboratory), Beijing, People's Republic of China and Institute of High Energy Physics, Academia Sinica, Beijing, People's Republic of China

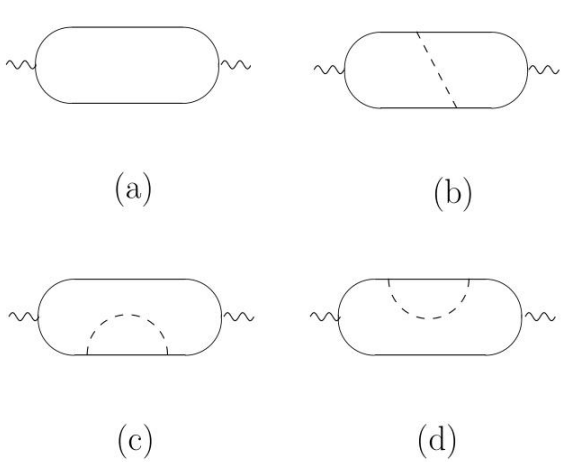
Zheng Huang
Institute of High Energy Physics, Academia Sinica, Beijing, People's Republic of China
(Received 23 June 1988)

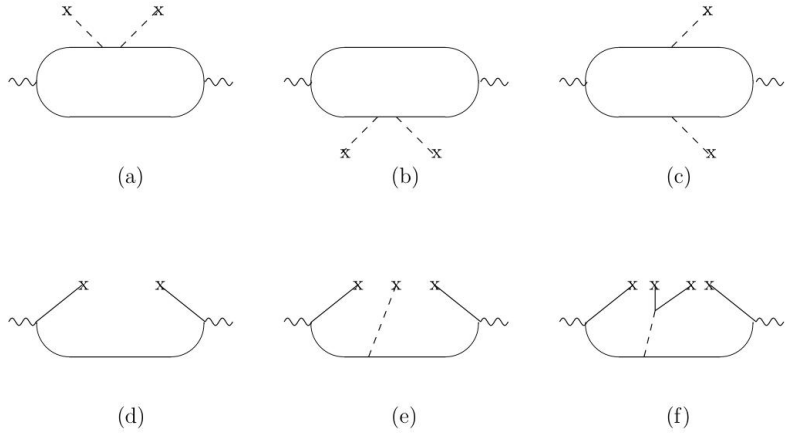
基于背景场系统展开凝聚项

$$A^a_\mu(x) \to A^a_\mu(x) + \phi^a_\mu(x)$$

$$\psi(x) \to \psi(x) + \eta(x)$$

QCD求和规则的基础构建恰当关联函数
Basis for QCD SR — In the $q^2<0$ space-like region





condensates contributions up to dimension-6

Free-quark loop and its NLO corrections

OPE-side

$$\Pi(q^2) = -\frac{1}{4\pi^2}\left(1+\frac{\alpha_s}{\pi}\right)\ln\frac{-q^2}{4m^2} + \frac{2m\langle\bar{\psi}\psi\rangle}{q^4} + \frac{\alpha_s\langle G^a_{\mu\nu}G^{a\mu\nu}\rangle}{12\pi q^4} + \frac{m^3}{3q^8}\langle g_s\bar{\psi}\sigma_{\mu\nu}\frac{\lambda^a}{2}G^{a\mu\nu}\psi\rangle + \frac{2\pi\alpha_s}{q^6}\left[\langle(\bar{\psi}\gamma_\mu\gamma_5\frac{\lambda^a}{2}\psi)(\bar{\psi}\gamma^\mu\gamma_5\frac{\lambda^a}{2}\psi)\rangle + \frac{2}{9}\langle(\bar{\psi}\gamma_\mu\frac{\lambda^a}{2}\psi)(\bar{\psi}\gamma^\mu\frac{\lambda^a}{2}\psi)\rangle\right]$$

Main SR features

Note: what's the value of α_s is one of its important error source (why fix $\mu \sim \sqrt{Q^2} \sim M$?)

QCD求和规则的基础构建恰当关联函数
Basis for QCD SR — values of vacuum condensates

$$\langle\bar{\psi}\psi\rangle = -\frac{f_\pi^2 m_\pi^2}{2(m_u+m_d)}$$

Semi-empirical, semi-phenomenological estimate
Dominant error sources for SR

凝聚项	典型数值	主要来源	精度
⟨q̄q⟩	−(235 MeV)³	GMOR 关系	±10%
⟨(αs/π)G²⟩	0.012 GeV⁴	charmonium 拟合	±50%
四夸克凝聚	~(1/N)⟨q̄q⟩²	因子化假设	±40%
六维胶子凝聚	~0.01 GeV⁶	瞬子模型	很差

$$\langle\bar{q}g_s\sigma Gq\rangle = m_0^2\langle\bar{q}q\rangle$$

$$m_0^2 \approx 0.8\mathrm{GeV}^2 \qquad \langle\bar{q}g_s\sigma Gq\rangle \approx -0.01\mathrm{GeV}^5$$

$$\langle\bar{q}q\rangle \approx -0.013\mathrm{GeV}^3$$

Dim-5 condensate

$$\langle(\bar{q}q)^2\rangle \approx \tfrac{1}{3}\langle\bar{q}q\rangle^2 \approx \tfrac{1}{3}\times(0.013)^2 \approx 5.6\times10^{-5}\mathrm{GeV}^6$$

常用数值范围：$\langle(\bar{q}q)^2\rangle \approx (3-8)\times10^{-5}\mathrm{GeV}^6$

$$\langle g_s^3G^3\rangle \approx (0.1-0.5)\mathrm{GeV}^2\times\langle G^2\rangle \approx (1.2-6)\times10^{-3}\mathrm{GeV}^6$$

Vacuum saturation hypothesis

SVZ 1979 年的拟合方法

Shifman、Vainshtein 和 Zakharov 用 **charmonium 求和规则**（J/ψ 和 ψ' 道）拟合给出经典值

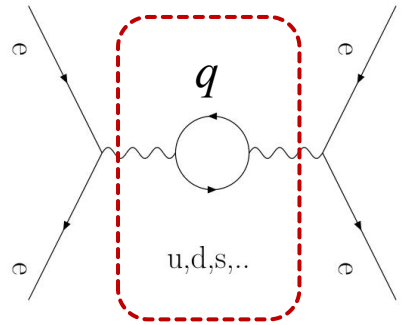
- **OPE 侧**：计算 charm 夸克圈的微扰贡献 + 胶子凝聚项
- **唯象侧**：用 J/ψ（3.097 GeV）和 ψ'（3.686 GeV）的实验峰位置和宽度
- **Borel 变换**：两侧都做 Borel 变换，在 Borel 窗口 $M^2 \approx 2-3\ \mathrm{GeV}^2$ 内匹配
- **拟合变量**：胶子凝聚值作为自由参数，拟合到实验谱

$$\left\langle\tfrac{\alpha_s}{\pi}G^2\right\rangle \approx 0.012\ \mathrm{GeV}^4$$

Main SR features

QCD求和规则的基础构建恰当关联函数
Basis for QCD SR — In the $q^2>0$ time-like region

Another side: $\sqrt{q^2} \to M_V$ with $V = \rho, \omega, \phi, j/\psi, \Upsilon, \cdots$



$q^2 > 0$ (类时 / 闵氏区)

中间态可以在壳，Im Π 非零

Using *unitarity relation* obtained by inserting a complete set of intermediate hadronic states

$\mathbf{1} = \sum_n \int d\tau_n \, |n\rangle\langle n|$

$$2\ \mathrm{Im}\,\Pi_{\mu\nu}(q) = \sum_n \int d\tau_n \, (2\pi)^4 \delta^{(4)}(q - p_n) \, \langle 0|j_\mu(0)|n\rangle\langle n|j_\nu(0)|0\rangle$$

$J^P = 1^-$

Single out the ground-state (or most important states) vector-meson contribution and introduce a compact notation for the rest of contributions (most uncertain)

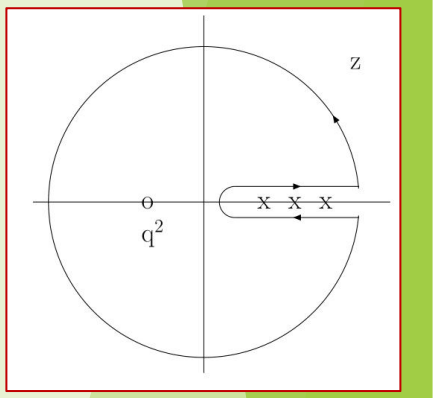
Hadronic-side

$$\frac{1}{\pi}\mathrm{Im}\ \Pi(q^2) = f_V^2 \delta(q^2 - m_V^2) + \rho^h(q^2)\theta(q^2 - s_0^h)$$

continuum threshold

hadron spectral function

QCD求和规则的基础构建恰当关联函数
Basis for QCD SR — Correlator has dual nature



To link both, using the Cauchy formulae

$$\Pi(q^2) = \frac{1}{2\pi i}\oint_C dz \frac{\Pi(z)}{z-q^2} = \frac{1}{2\pi i}\oint_{|z|=R} dz \frac{\Pi(z)}{z-q^2} + \frac{1}{2\pi i}\int_0^R dz \frac{\Pi(z+i\epsilon)-\Pi(z-i\epsilon)}{z-q^2}$$

$\oint_C = \oint_{|z|=R} + \int_{上岸} + \int_{下岸}$

足够快地衰减：$\Pi(z) \sim \frac{1}{|z|^\epsilon},\ \epsilon > 0$

阈值 $s_0 \to 0$

Using Schwartz reflection principle

$$\Pi(z+i\epsilon) - \Pi(z-i\epsilon) = \Pi(z+i\epsilon) - [\Pi(z+i\epsilon)]^* = 2i\ \mathrm{Im}\,\Pi(z+i\epsilon)$$

$$\Pi(q^2) = \frac{1}{\pi}\int_{t_{min}}^{\infty} ds \frac{\mathrm{Im}\ \Pi(s)}{s-q^2-i\epsilon} \qquad t_{min} = \min\{m_V^2, s_0^h\}$$

QCD求和规则的基础构建恰当关联函数
Basis for QCD SR — Correlator has dual nature

If the correlator does not vanish at $q^2 \to \infty$

Define a new correlator
free of divergence and be less uncertain

$$\bar{\Pi}(q^2) = \Pi(q^2) - \Pi(0) = \frac{q^2}{\pi}\int_{t_{\min}}^{\infty} ds\, \frac{\mathrm{Im}\,\Pi(s)}{s(s-q^2)}$$

$$\Pi(q^2) = \frac{q^2 f_V^2}{m_V^2(m_V^2 - q^2)} + q^2 \int_{s_0^h}^{\infty} ds \frac{\rho^h(s)}{s(s-q^2)} + \Pi(0)$$

Not unique
But effective

Doing Borel transformation to suppress unknown contributions

$$\Pi(M^2) \equiv \mathcal{B}_{M^2}\Pi(q^2) = \lim_{\substack{-q^2,n\to\infty \\ -q^2/n=M^2}} \frac{(-q^2)^{(n+1)}}{n!}\left(\frac{d}{dq^2}\right)^n \Pi(q^2)$$

Main SR features

QCD求和规则的基础构建恰当关联函数
Basis for QCD SR — the resultant precise sum rules

$$\Pi(M^2) = f_V^2 e^{-m_V^2/M^2} + \int_{s_0^h}^{\infty} ds\, \rho^h(s) e^{-s/M^2}$$

Thus the Borel transformation removes subtraction terms in the dispersion relation and exponentially suppresses the contributions from excited resonances and continuum states heavier than V

quark-hadron duality

$$\mathrm{Im}\,\Pi(s) \to \mathrm{Im}\,\Pi^{(pert)}(s) \quad \text{at } s \to +\infty$$

$$\int_{s_0^h}^{\infty} ds\, \rho^h(s) e^{-s/M^2} \simeq \frac{1}{\pi} \int_{s_0}^{\infty} ds\, \mathrm{Im}\,\Pi^{(pert)}(s) e^{-s/M^2}$$

Approx.: condensate contributions are power suppressed and negligible

$$\mathrm{Im}\,\Pi^{(0)}(s) = \tfrac{1}{8\pi} v(3-v^2)\theta(s-4m^2)$$

$$\mathrm{Im}\,\Pi^{(pert)}(s) = \mathrm{Im}\,\Pi^{(0)}(s)\left\{1 + \alpha_s C_F\left[\frac{\pi}{2v} - \frac{v+3}{4}\left(\frac{\pi}{2} - \frac{3}{4\pi}\right)\right]\right\}$$

速度 $v = \sqrt{1-4m^2/s}$

Main SR features

QCD求和规则的基础构建恰当关联函数
Basis for QCD SR — the resultant precise sum rules

$$f_V^2 e^{-m_V^2/M^2} + \int_{s_0^h}^{\infty} ds\ \rho^h(s) e^{-s/M^2} = \frac{1}{4\pi^2}\left(1+\frac{\alpha_s(M)}{\pi}\right)\int_0^{\infty} ds\ e^{-s/M^2} + \frac{2m\langle\bar{\psi}\psi\rangle}{M^2} + \frac{\langle\frac{\alpha_s}{\pi}G^a_{\mu\nu}G^{a\mu\nu}\rangle}{12M^2} - \frac{112\pi}{81}\frac{\alpha_s\langle\bar{\psi}\psi\rangle^2}{M^4}$$

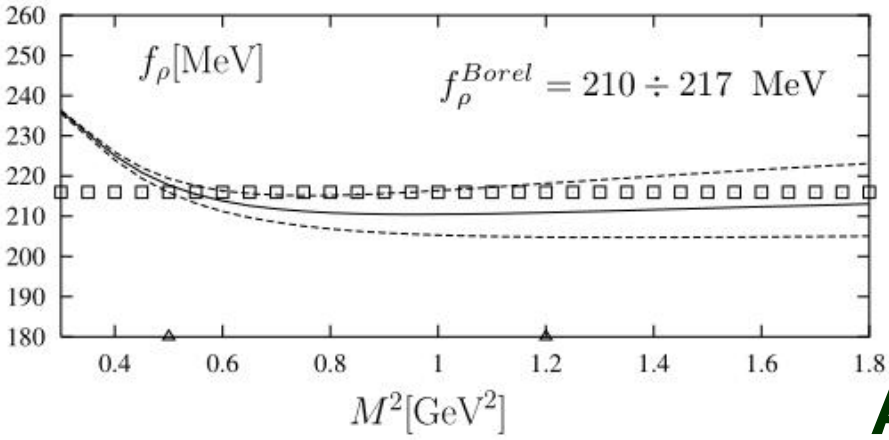
$$\int_{s_0^h}^{\infty} ds\,\rho^h(s)e^{-s/M^2} \simeq \frac{1}{\pi}\int_{s_0}^{\infty} ds\,\mathrm{Im}\,\Pi^{(pert)}(s)e^{-s/M^2}$$

Note: $s_0 \approx s^h{}_o$, not necessarily be coincide. One of the error source, expected to be close to the mass squared of the first excited state - usual criteria: flatness

Final sum rule up to dimension-4 for the rho-meson decay constant

$$f_\rho^2 = M^2 e^{m_\rho^2/M^2}\left[\frac{1}{4\pi^2}\left(1-e^{-s_0^\rho/M^2}\right)\left(1+\frac{\alpha_s(M)}{\pi}\right)+\frac{(m_u+m_d)\langle\bar{\psi}\psi\rangle}{M^4}+\frac{1}{12}\frac{\langle\frac{\alpha_s}{\pi}G^a_{\mu\nu}G^{a\mu\nu}\rangle}{M^4}-\frac{112\pi}{81}\frac{\alpha_s\langle\bar{\psi}\psi\rangle^2}{M^6}\right]$$

Main SR features



S_0=1.7 GeV²

0.5 > M^2 > 1.2 GeV²

d=6 condensate < 10%

continuum above s_0 < 30%

Sum rules are approximate relations
But helpful and deserve continued studies

QCD求和规则方法总结
A simple discussion of SR procedures

Several approximations has been for deriving the sum rules, and the accurateness of the QCD sum rules inversely heavily depends on the preciseness of those approximations

Borel window

- The low limit of M^2 is usually fixed by demanding that **the condensate term with the highest dimension remains a small fraction of sum of all terms**, which makes the convergence of condensate expansion under well control
- At too large M^2, the quark-hadron duality approximation cannot be trusted. Therefore, the upper limit on M^2, should make **the contribution of the states above s_0 be a small part of the total dispersion integral**
- Physical observable should not depend on the manly input parameters. Thus, **the prediction should be flat versus the input parameter of Borel parameter** within the allowable Borel

精度有限，方法本身也有完善空间；但仍不失为有效手段

2. The sum rules for the light-meson LCDAs (BFTSR)

Why LCDA, basic idea of LCSR approach

SVZ sum rule employs 【vacuum-to-vacuum】 correlator
LCSR adopts 【vacuum-to-on-shell state】 correlator

The basic idea of LCSR is to expand the products of currents near the light-cone. It involves a partial resummation of local operators and avoids certain irregularities of the truncated OPE in usual **three-point sum rules** for two bound-state transitions

$$\Pi(p_1,p_2)=\int dx\,dy\,e^{-ip_1x+ip_2y}\,\langle 0|T\{H_2(y)\,J(0)\,H_1(x)\}|0\rangle$$

$$\int dx\,dy\,e^{-ip_1x+ip_2y}\langle 0|T\{H_2(y)J(0)H_1(x)\}|0\rangle\sim\langle 0|H_2|h_2\rangle\,\frac{1}{m_2^2-p_2^2}\,\langle h_2|J|h_1\rangle\,\frac{1}{m_1^2-p_1^2}\,\langle h_1|H_1|0\rangle$$

Serious problems of three-point SVZ sum rules

$$\int_{R_{12}} ds\,ds'\frac{\rho^h(s,s')}{(s-p^2)(s'-p'^2)}$$

- OPE upsets powercounting in the large momentum/mass
- Contamination of the sum rule by "**nondiagonal**" transitions of the ground state to excited state (have to introduce double dispersion relations; double Borel transformation;…)

Why LCDAs Are Organized by Twist

At high Q^2, lower twist dominates, higher twist suppressed by powers

Definition · twist $t = d - s$; s is the Lorentz rank of the operator

Ordering · γ_μ gives twist-2; $1, \gamma_5, \sigma_{\mu\nu}$ gives twist-3

Normalization · Each twist is normalized to $\int_0^1 dx\ \varphi(x) = 1$;
twist-2 carries f_P, twist-3 carries $f_P \mu_P$ with $\mu_P = m_P^2/(m_u + m_d)$

Benefits of the twist expansion

Systematic expansion twist-2 → 3 → 4, each step suppressed by $(\Lambda/Q)^{t-2}$	**Factorizable** hard part and the soft LCDA separate cleanly	**Universal LCDAs** one per twist, extractable from lattice, sum rules or experiment	**Clear picture** twist-2 dominates, higher twist is a correction, easy to size up	**Controlled error** truncation at a given twist, error estimated by power counting

Pion leading-twist distribution amplitude

Definition. Leading-twist LCDA parameterizes the nonlocal quark-flavor matrix element on the light cone:

$$\left\langle 0\left|\bar{d}(0)\gamma_\mu\gamma_5[0,z]u(z)\right|\pi(q)\right\rangle = if_\pi q_\mu \int_0^1 dx\; e^{i(x\,q\cdot z)}\phi_\pi(x,\mu)$$

Why it matters. The LCDA is universal nonperturbative input to factorization theorems for hard exclusive processes

Gegenbauer expansion. At any scale μ, it is usually expanded as

$$\phi_\pi(x,\mu) = 6x(1-x)\left[1+\sum_{n=2,4,\ldots} a_n^\pi(\mu)C_n^{3/2}(2x-1)\right]$$

The moments are: $\langle \xi^n\rangle = \int_0^1 dx\;(2x-1)^n\phi_\pi(x,\mu)$

Asymptotic limit: all $a_n^\pi = 0$, giving $\phi_\pi^{as}(x) = 6x(1-x)$ with $\langle\xi^2\rangle = 0.2$.

$$a_2^\pi = \frac{7}{12}(5\langle\xi^2\rangle - 1),$$

$$a_4^\pi = -\frac{11}{24}(14\langle\xi^2\rangle - 21\langle\xi^4\rangle - 1),$$

$$a_6^\pi = \frac{5}{64}(135\langle\xi^2\rangle - 495\langle\xi^4\rangle + 429\langle\xi^6\rangle - 5)$$

Moments can be calculated by using BFTSR approach

Pion leading-twist distribution amplitude

Correlator

$$\Pi_\pi^{(n,0)}(z,q) = i\int d^4x e^{iq\cdot x}\langle 0|T\{J_n(x)J_0^\dagger(0)\}|0\rangle = (z\cdot q)^{n+2} I_\pi^{(n,0)}(q^2)$$

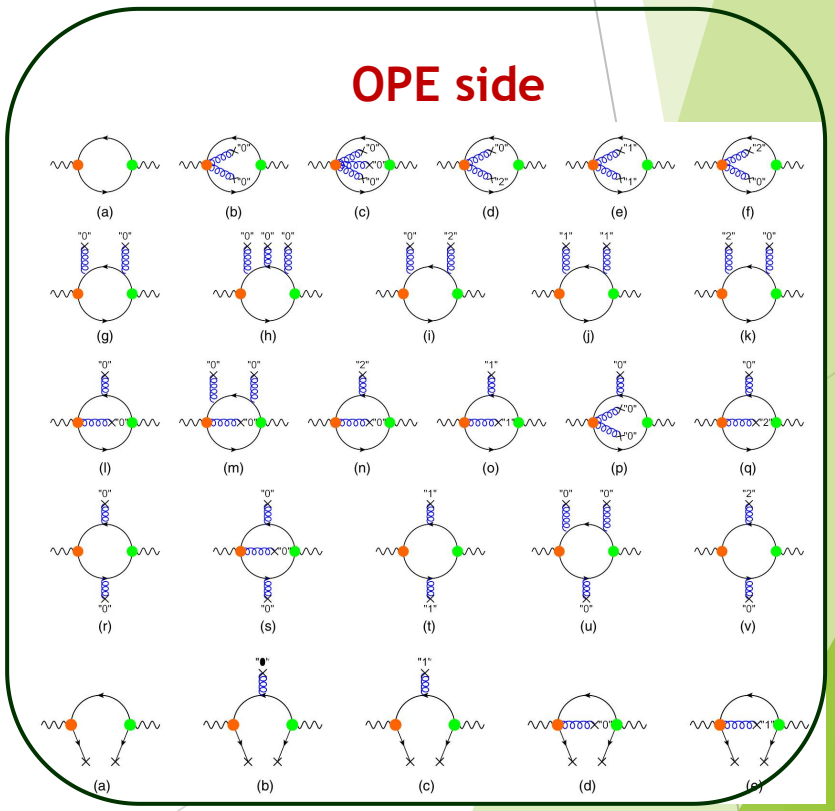
$$J_n(x) = \bar{d}(x)\not{z}\gamma_5(iz\cdot \overleftrightarrow{D})^n u(x)$$

Hadronic side

$$\langle 0|\bar{d}(0)\not{z}\gamma_5(iz\cdot \overleftrightarrow{D})^n u(0)|\pi(q)\rangle = i(z\cdot q)^{n+1} f_\pi \langle \xi^n\rangle$$

$$\mathrm{Im}\,\Pi_{\pi,\mathrm{had}}^{(n,0)}(q^2) = \pi\,\delta(q^2-m_\pi^2)\,f_\pi^2\,\langle\xi^n\rangle \;+\; \pi\frac{3}{4\pi^2(n+1)(n+3)}\,\theta(q^2-s_\pi)$$

OPE side



Phys. Rev. D 90, 016004 (2014)

Pion leading-twist distribution amplitude

$$\frac{\langle \xi^n\rangle_{2;\pi}\ \langle \xi^0\rangle_{2;\pi}\ f_\pi^2}{M^2 e^{m_\pi^2/M^2}} = \frac{3}{4\pi^2}\frac{1}{(n+1)(n+3)}(1-e^{-s_\pi/M^2}) + \frac{(m_d+m_u)\langle\bar{q}q\rangle}{(M^2)^2} + \frac{\langle\alpha_s G^2\rangle}{(M^2)^2}\frac{1+n\theta(n-2)}{12\pi(n+1)}$$
$$-\frac{(m_d+m_u)\langle g_s\bar{q}\sigma TGq\rangle}{(M^2)^3}\frac{8n+1}{18} + \frac{\langle g_s\bar{q}q\rangle^2}{(M^2)^3}\frac{4(2n+1)}{81} - \frac{\langle g_s^3 fG^3\rangle}{(M^2)^3}\frac{n\theta(n-2)}{48\pi^2} + \frac{\langle g_s^2\bar{q}q\rangle^2}{(M^2)^3}\frac{2+\kappa^2}{486\pi^2}$$
$$\times\left\{-2(51n+25)\left(-\ln\frac{M^2}{\mu^2}\right) + 3(17n+35) + \theta(n-2)\left[2n\left(-\ln\frac{M^2}{\mu^2}\right) + \frac{49n^2+100n+56}{n}\right.\right.$$
$$\left.\left. - 25(2n+1)\left[\psi\left(\frac{n+1}{2}\right) - \psi\left(\frac{n}{2}\right) + \ln 4\right]\right]\right\}$$

$$\frac{\langle \xi^0\rangle_{2;\pi}^2\ f_\pi^2}{M^2 e^{m_\pi^2/M^2}} = \frac{1}{4\pi^2}\left(1+\frac{\alpha_s}{\pi}\right)(1-e^{-s_\pi/M^2}) + (m_d + m_u)\frac{\langle\bar{q}q\rangle}{(M^2)^2} + \frac{\langle\alpha_s G^2\rangle}{(M^2)^2}\frac{1}{12\pi} - \frac{1}{18}(m_d+m_u)$$
$$\times\frac{\langle g_s\bar{q}\sigma TGq\rangle}{(M^2)^3} + \frac{4}{81}\frac{\langle g_s\bar{q}q\rangle^2}{(M^2)^3} + \frac{\langle g_s^2\bar{q}q\rangle^2}{(M^2)^3}\frac{2+\kappa^2}{486\pi^2}$$
$$\times\left[-50\left(-\ln\frac{M^2}{\mu^2}\right) + 105\right]$$

One minor point: Normalization

$\langle \xi^0\rangle = \int_0^1 dx\ \phi_\pi(x,\mu) = 1$

$$\langle \xi^n\rangle_{2;\pi}|_\mu = \frac{(\langle \xi^n\rangle_{2;\pi}|_\mu \langle \xi^0\rangle_{2;\pi}|_\mu)|_{\text{From Eq. (7)}}}{\sqrt{\langle \xi^0\rangle_{2;\pi}^2|_\mu}|_{\text{From Eq. (10)}}}$$

Directly transform back to Gegenbauer form ?

Gegenbauer 展开是正交基展开，而非渐近展开

更多矩不等于更精确——形状应由物理约束确定

Pion leading-twist distribution amplitude

$\Psi_{c.m.}(q) \propto exp(-q^2/2\beta^2) \Rightarrow$ BHL-model

$\Psi^R(x, k_\perp) \propto exp[-(k_\perp^2+m_q^2)/(8\beta^2 x(1-x))]$

$$\Psi^R_{2;\pi}(x, \mathbf{k}_\perp) = A_{2;\pi}\varphi_{2;\pi}(x) \exp\left[-\frac{\mathbf{k}_\perp^2 + m_q^2}{8\beta^2_{2;\pi} x\bar{x}}\right]$$

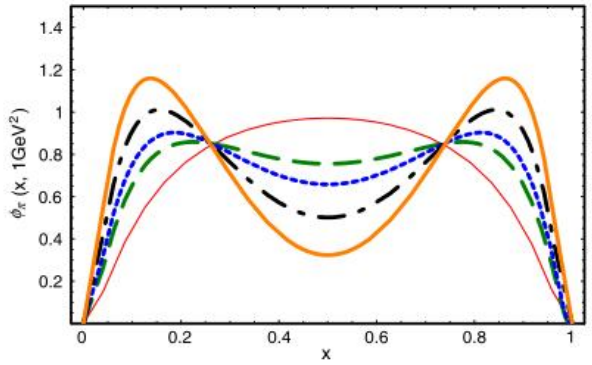


FIG. 4 (color online). The pion leading-twist DA versus the parameter B at $\mu = 1$ GeV, where the thin-solid, dashed, dotted, dash-dotted, and thick-solid lines are $B = 0.01$, 0.14, 0.2, 0.3, and 0.42, respectively.

Phys. Rev. D 88, 034013 (2013)

$$\varphi^{\rm I}_{2;\pi}(x) = 1 + B \times C_2^{3/2}(2x-1).$$

$$\varphi^{\rm II}_{2;\pi}(x) = 1 + B_2 \times C_2^{3/2}(2x-1) + B_4 \times C_4^{3/2}(2x-1)$$

$$\varphi^{\rm III}_{2;\pi}(x) = [x\bar{x}]^{a_{2;\pi}}$$

$$\varphi^{\rm IV}_{2;\pi}(x) = [x\bar{x}]^{a_{2;\pi}}[1 + \hat{a}_2^{2;\pi} C_2^{3/2}(2x-1)]$$

Improved by combining the measured data

Phenomenological model from BFTSR to LCHO

1. **QCDSR constraints** on the first few moments $\langle \xi^2 \rangle$, $\langle \xi^4 \rangle$, $\langle \xi^6 \rangle$
2. **LCHO model** to parameterize the DA shape
3. **Experimental TFF data** from BABAR, BELLE, CLEO, CELLO to further constrain the DA via the pion-photon transition form factor

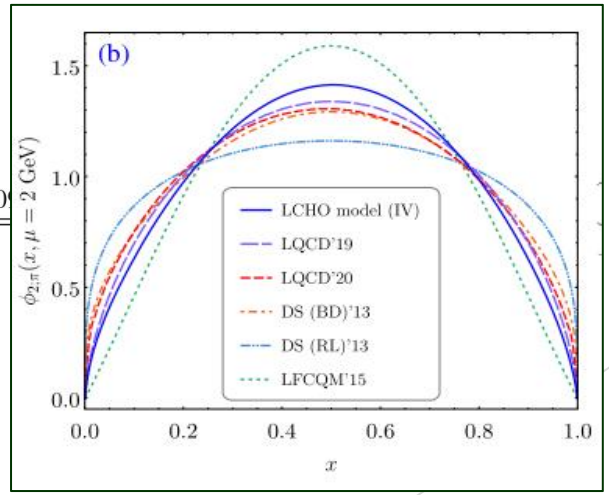
Phys. Rev. D 104, 016021 (2021)

Pion leading-twist distribution amplitude

TABLE III. Our predictions for the first five nonvanishing moments and inverse moment of the pion DA, compared to other theoretical predictions. The values obtained using the formula combining Eqs. (7) and (9) are also shown.

	μ[GeV]	$\langle\xi^2\rangle_{2;\pi}\vert_\mu$	$\langle\xi^4\rangle_{2;\pi}\vert_\mu$	$\langle\xi^6\rangle_{2;\pi}\vert_\mu$	$\langle\xi^8\rangle_{2;\pi}\vert_\mu$	$\langle\xi^{10}\rangle_{2;\pi}\vert_\mu$	$\langle x^{-1}\rangle\vert_\mu$
BFTSR (this work)	1	0.271(13)	0.138(10)	0.087(6)	0.064(7)	0.050(6)	3.95
BFTSR (this work)	2	0.254(10)	0.125(7)	0.077(6)	0.054(5)	0.041(4)	3.33
Asymptotic	∞	0.200	0.086	0.048	0.030	0.021	3.00
LF holographic ($B=0$) [54]	1,2	0.180, 0.185	0.067, 0.071	…	…	…	2.81,2.85
LF holographic ($B\gg1$) [54]	1,2	0.200, 0.200	0.085, 0.085	…	…	…	2.93,2.95
LF holographic [55]	~1	0.237	0.114	…	…	…	4.0
Platykurtic [56]	2	$0.220^{+0.009}_{-0.006}$	$0.098^{+0.008}_{-0.005}$	…	…	…	$3.13^{+0.14}_{-0.10}$
LF quark model [57]	~1	0.24(22)	0.11(9)	…	…	…	…
Sum rules [58]	1	0.24	0.11	…	…	…	…
Renormalon model [59]	1	0.28	0.13	…	…	…	…
Instanton vacuum [60,61]	1	0.22, 0.21	0.10,0.09	…	…	…	…
NLC sum rules [62]	2	$0.248^{+0.016}_{-0.015}$	$0.108^{+0.05}_{-0.03}$	…	…	…	3.16(9)
Sum rules [5]	2	0.343	0.181	…	…	…	4.25
Dyson-Schwinger [RL,DB] [14]	2	0.280, 0.251	0.151, 0.128	…	…	…	5.5,4.6
Lattice [63]	2	0.28(1)(2)	…	…			
Lattice [64]	2	0.2361(41)(39)	…	…			
Lattice [65]	2	0.27(4)	…	…			
Lattice [66]	2	0.2077(43)	…	…			
Lattice [67]	2	0.234(6)(6)	…	…			
Lattice [68]	2	0.244(30)	…	…			
Eq. (7) + Eq. (9)	1	0.303(19)	0.179(21)	0.128(16)	0.0		

$$\langle x^{-1}\rangle\vert_\mu = \int_0^1 dx x^{-1}\phi_{2;\pi}(x,\mu)$$



Phys. Rev. D 104, 016021 (2021)

Eur. Phys. J. C (2016) 76:390

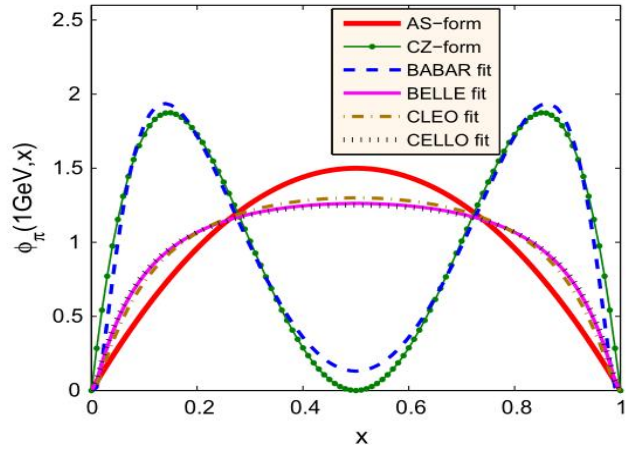


Fig. 9 The pion DAs with the parameters listed in Table 1, which are fit from the TFF data of BABAR, BELLE, CLEO, and CELLO Collaborations, respectively. As a comparison, we also present the asymptotic-DA [6] and the CZ-DA [36] in the figure

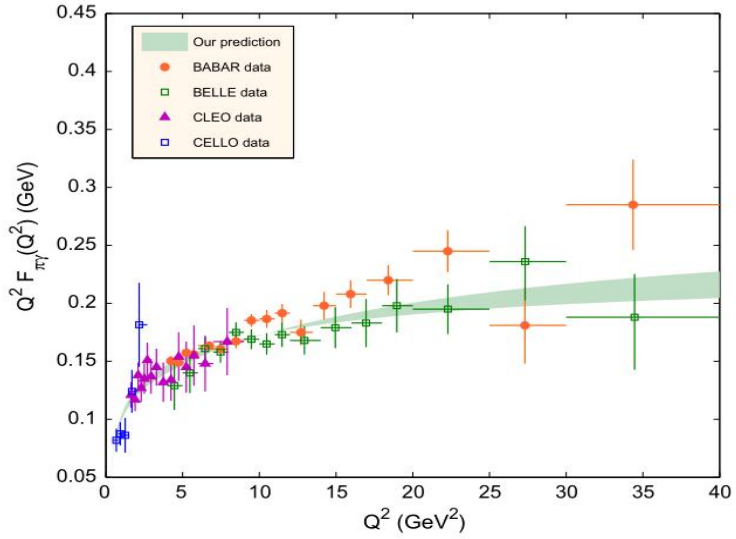


Fig. 10 The predicted pion–photon TFF $Q^2F_{\pi\gamma}(Q^2)$ by using the parameters determined from the BELLE and the CLEO data. The BABAR, the BELLE, the CLEO, and the CELLO data are also presented as a comparison

Following the same SR procedures, η/η'-leading twist DA

Eur. Phys. J. C (2022) 82:12
https://doi.org/10.1140/epjc/s10052-021-09958-0

THE EUROPEAN PHYSICAL JOURNAL C

Regular Article - Theoretical Physics

$\eta^{(\prime)}$-meson twist-2 distribution amplitude within QCD sum rule approach and its application to the semi-leptonic decay $D_s^+ \to \eta^{(\prime)}\ell^+\nu_\ell$

Dan-Dan Hu[1], Hai-Bing Fu[1,3,a], Tao Zhong[1], Long Zeng[2,3], Wei Cheng[4], Xing-Gang Wu[2,3,b]

Eur. Phys. J. C (2024) 84:15
https://doi.org/10.1140/epjc/s10052-023-12333-w

THE EUROPEAN PHYSICAL JOURNAL C

Regular Article - Theoretical Physics

Properties of the η_q leading-twist distribution amplitude and its effects to the $B/D^+ \to \eta^{(\prime)}\ell^+\nu_\ell$ decays

Dan-Dan Hu[1,a], Xing-Gang Wu[1,b], Hai-Bing Fu[2,c], Tao Zhong[2,d], Zai-Hui Wu[2,e], Long Zeng[1,f]

Using the simple quark-flavor basis

$$|\eta\rangle = \cos\varphi|\eta_q\rangle - \sin\varphi|\eta_s\rangle \qquad |\eta_q\rangle = |\bar{u}u+\bar{d}d\rangle/\sqrt{2}$$
$$|\eta'\rangle = \sin\varphi|\eta_q\rangle + \cos\varphi|\eta_s\rangle \qquad |\eta_s\rangle = |\bar{s}s\rangle$$

$$D_s^+ \to \eta^{(\prime)}\ell^+\nu_\ell$$

$$f_+^{B(D)\to\eta} = \cos\phi f_+^{B(D)\to\eta_q}$$
$$f_+^{B(D)\to\eta'} = \sin\phi f_+^{B(D)\to\eta_q}$$

$$\begin{pmatrix} |\eta\rangle \\ |\eta'\rangle \end{pmatrix} = \begin{pmatrix} \cos\phi & -\sin\phi \\ \sin\phi & \cos\phi \end{pmatrix} \begin{pmatrix} |\eta_q\rangle \\ |\eta_s\rangle \end{pmatrix}$$

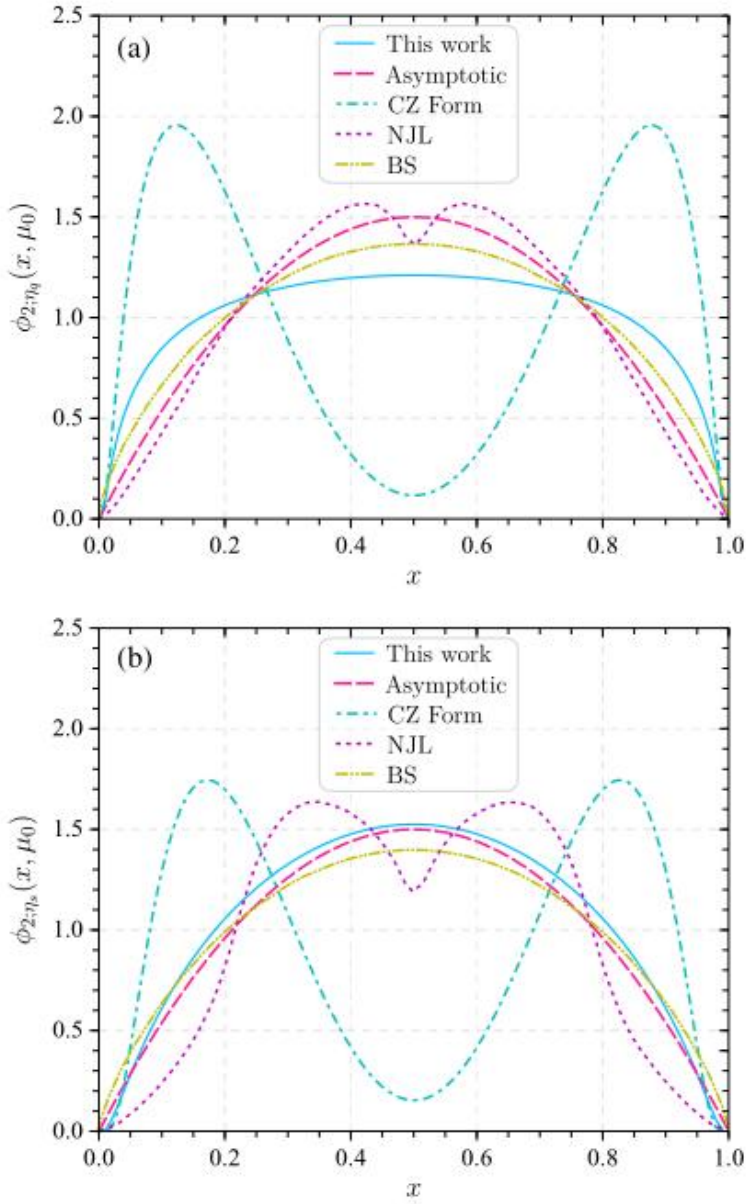


FIG. 2. η_q and η_s mesons' leading-twist LCDAs $\phi_{2;\eta_q}(x,\mu_0)$(a) and $\phi_{2;\eta_s}(x,\mu_0)$(b) with $\mu_0 = 1$ GeV. As a comparison, the curves from the nonlocal NJL model [29], the BS model [31],

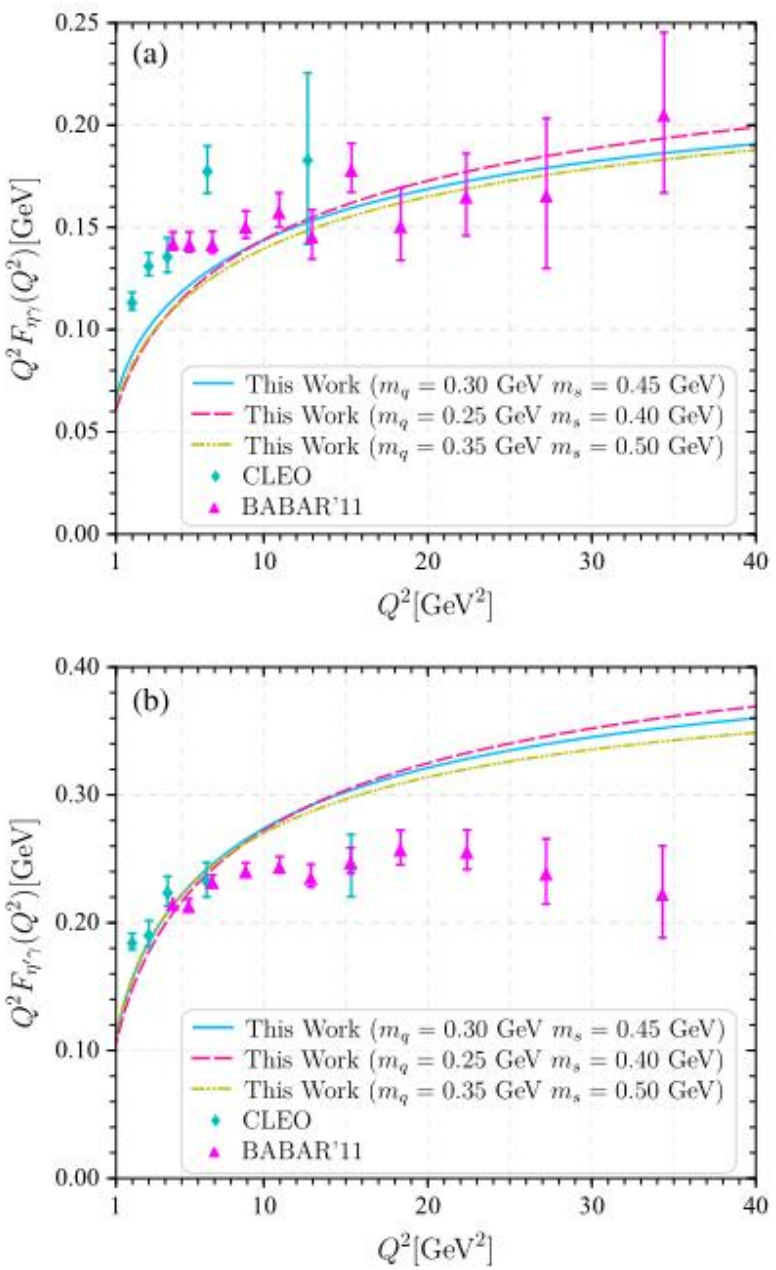


FIG. 4. $\eta-\gamma$ and $\eta'-\gamma$ TFFs $Q^2F_{\eta\gamma}(Q^2)$ (a) and $Q^2F_{\eta'\gamma}(Q^2)$ (b) are calculated for different mixing angles. The experimental results of CLEO [20] and *BABAR*'11 [21] are also represented.

Phys. Rev. D 114, 016003 (2026)

Taking into possible intrinsic charm

$$\begin{pmatrix} |\eta\rangle \\ |\eta'\rangle \\ |\eta_c\rangle \end{pmatrix} = U(\theta,\theta_c,\theta_i) \begin{pmatrix} |\eta_q\rangle \\ |\eta_s\rangle \\ |\eta_{c_0}\rangle \end{pmatrix},$$

$$U(\theta,\theta_c,\theta_i) = \begin{pmatrix} 0.7611 & -0.6486 & -0.0044 \\ 0.6484 & 0.7611 & -0.0173 \\ 0.0146 & 0.0103 & 0.9998 \end{pmatrix}$$

$$f_{\eta_{c_0}} = -f^c_{\eta'_c}/0.0173.$$

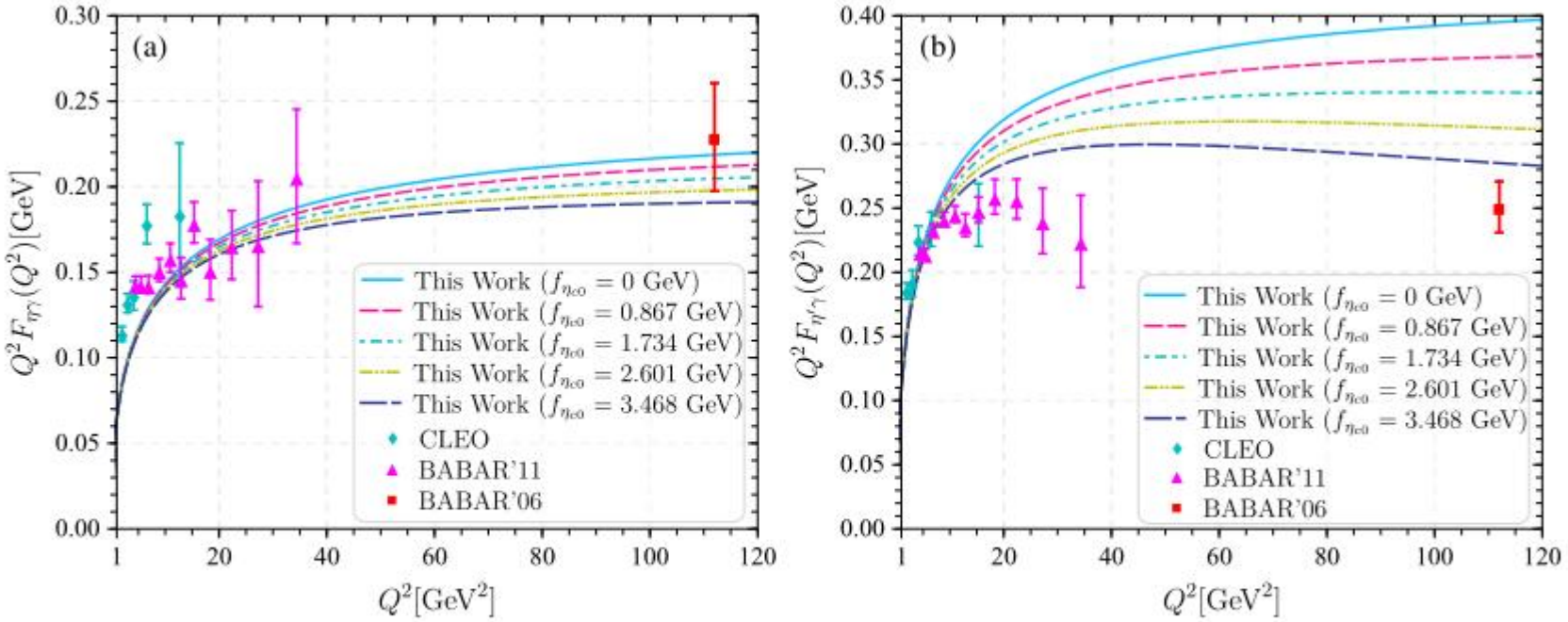


FIG. 5. $\eta-\gamma$ and $\eta'-\gamma$ TFFs $Q^2F_{\eta\gamma}(Q^2)$ (a) and $Q^2F_{\eta'\gamma}(Q^2)$ (b) are obtained through $\eta-\eta'-\eta_c$ mixing mechanism. The experimental results from CLEO [20], *BABAR*'11 [21], and *BABAR*'06 [22] are also represented.

Phys. Rev. D 112, 076001 (2025) ; Phys. Rev. D 114, 016003 (2026)

Further taking into possible gluonic component

$$\begin{pmatrix} |\eta\rangle \\ |\eta'\rangle \\ |G\rangle \\ |\eta_c\rangle \end{pmatrix} = U(\theta,\phi_g,\phi_c,\theta_g) \begin{pmatrix} |\eta_q\rangle \\ |\eta_s\rangle \\ |gg\rangle \\ |\eta_{c_0}\rangle \end{pmatrix}$$

$$U(\theta,\phi_g,\phi_c,\theta_g) = \begin{pmatrix} 0.7517 & -0.6595 & -0.0005 & -0.0049 \\ 0.6593 & 0.7516 & -0.0023 & -0.0206 \\ 0.0019 & 0.0013 & 1.000 & -0.0001 \\ 0.0173 & 0.0122 & 0.0001 & 0.9998 \end{pmatrix}$$

$$f_{\eta_{c_0}} = -f^c_{\eta'_c}/0.0173.$$

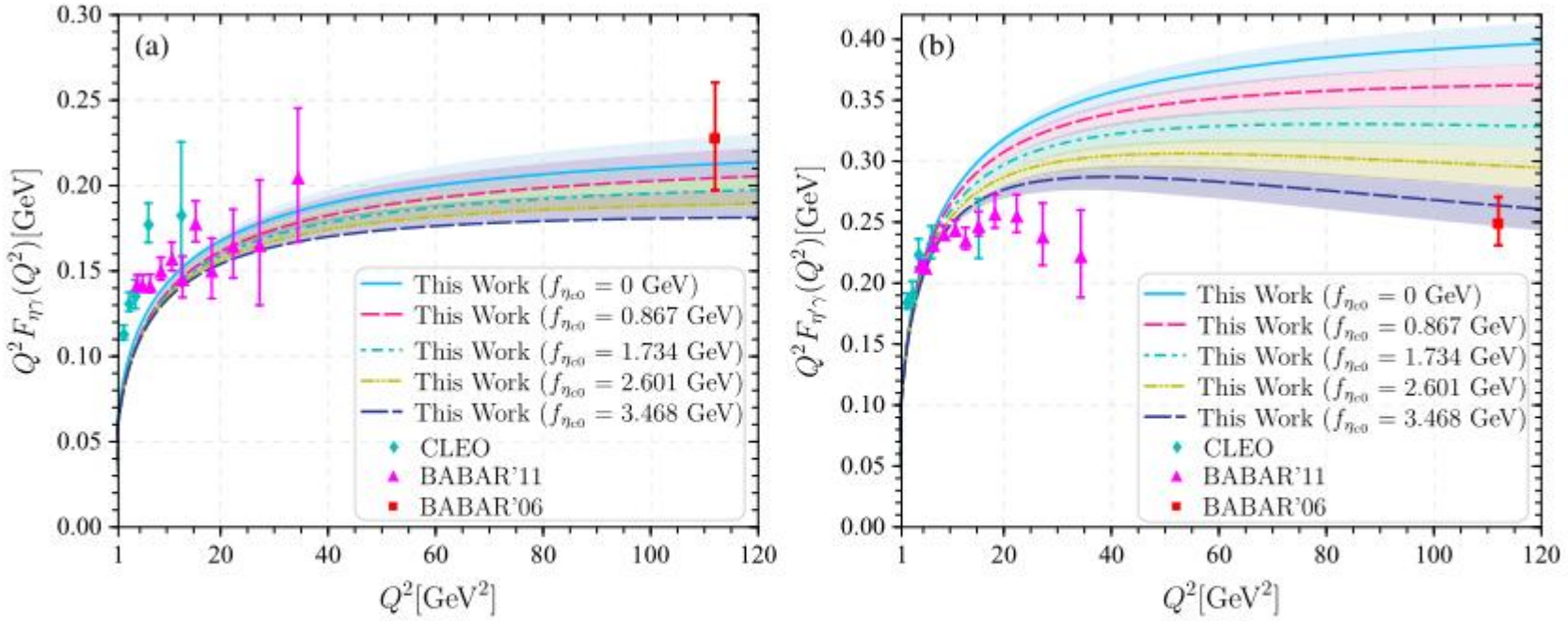


FIG. 6. $\eta-\gamma$ and $\eta'-\gamma$ TFFs $Q^2F_{\eta\gamma}(Q^2)$ (a) and $Q^2F_{\eta'\gamma}(Q^2)$ (b) are obtained through $\eta-\eta'-G-\eta_c$ mixing mechanism, which the shaded band indicates as the uncertainty arising from different choices of light constituent quark masses (e.g., $m_q = 0.30 \pm 0.05$ GeV and $m_s = 0.45 \pm 0.05$ GeV). The experimental results from CLEO [20], *BABAR*'11 [21] and *BABAR*'06 [22] are also represented.

Phys. Rev. D 112, 076001 (2025) ; Phys. Rev. D 114, 016003 (2026)

Taking into possible gluonic component

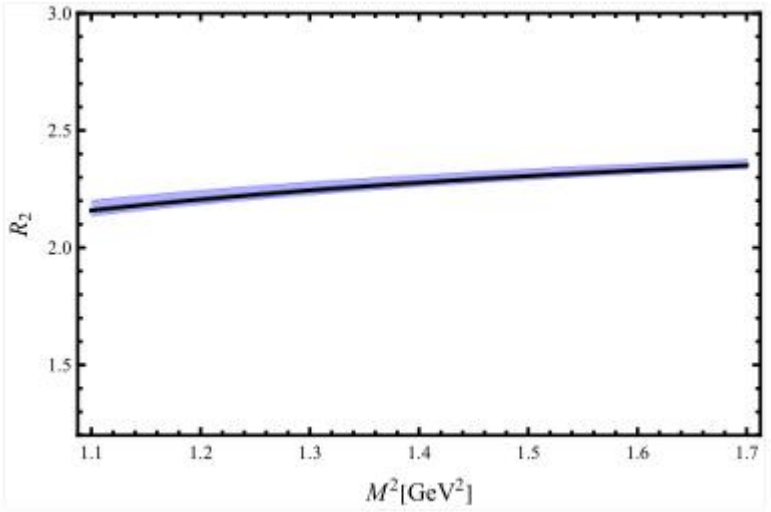
$$\begin{pmatrix} |\eta\rangle \\ |\eta'\rangle \\ |G\rangle \end{pmatrix} = U(\theta, \phi_G, \theta_i) \begin{pmatrix} |\eta_q\rangle \\ |\eta_s\rangle \\ |g\rangle \end{pmatrix}$$

Initial results

$$\frac{m_\eta^2 s\theta s\phi_G(s\theta s\theta_i c\phi_G - c\theta c\theta_i) + m_{\eta'}^2 c\theta s\phi_G(c\theta s\theta_i c\phi_G + s\theta c\theta_i) - m_G^2 s\theta_i s\phi_G c\phi_G}{m_\eta^2 s\theta s\phi_G(s\theta c\theta_i c\phi_G + c\theta s\theta_i) + m_{\eta'}^2 c\theta s\phi_G(c\theta c\theta_i c\phi_G - s\theta s\theta_i) - m_G^2 c\theta_i s\phi_G c\phi_G} = \frac{\sqrt{2} f_{\eta_s}}{f_{\eta_q}}$$

⇦ SR

$$R_2 \equiv \left(\frac{\sqrt{2} f_{\eta_s}}{f_{\eta_q}}\right)^2 \qquad R_2 = 2e^{(m_{\eta_s}^2 - \bar{m}_{\eta_q}^2)/M^2} \left\{ \frac{\mathcal{P}_s}{\mathcal{P}_q} + \frac{\mathcal{P}_q \mathcal{C}_{s,4} - \mathcal{P}_s \mathcal{C}_{q,4}}{\mathcal{P}_q^2} + \frac{\mathcal{P}_s \mathcal{C}_{q,4}^2 - \mathcal{P}_q \mathcal{C}_{s,4} \mathcal{C}_{q,4} - \mathcal{P}_s \mathcal{P}_q \mathcal{C}_{q,6} + \mathcal{P}_q^2 \mathcal{C}_{s,6}}{\mathcal{P}_q^3} \right\},$$



$$\mathcal{P}_q = \frac{1}{4\pi^2}\left(1 + \frac{\alpha_s}{\pi} A_0'\right)\left(1 - e^{-s_{\eta_q}/M^2}\right),$$

$$\mathcal{P}_s = \frac{1}{8\pi^2 M^2} \int_{4m_s^2}^{s_{\eta_s}} ds\, e^{-s/M^2}\, v(3 - v^2)\left(1 + \frac{\alpha_s}{\pi} A_0'\right),$$

$$\mathcal{C}_{q,4} = \frac{(m_u + m_d)\langle \bar{q}q \rangle}{M^4} + \frac{\langle \alpha_s G^2 \rangle}{12\pi M^4},$$

$$\mathcal{C}_{s,4} = \frac{2m_s \langle \bar{s}s \rangle}{M^4} + \frac{\langle \alpha_s G^2 \rangle}{12\pi M^4},$$

$$\mathcal{C}_{q,6} = -\frac{(m_u + m_d)\langle g_s \bar{q}\sigma TGq \rangle}{18M^6} + \frac{4\langle g_s \bar{q}q \rangle^2}{18M^6} + \frac{(2 + \kappa^2)\langle g_s^2 \bar{q}q \rangle^2}{486\pi^2 M^6}\left(-50\left(-\ln\frac{M^2}{\mu^2}\right) + 105\right),$$

$$\mathcal{C}_{s,6} = -\frac{m_s \langle g_s \bar{s}\sigma TGs \rangle}{9M^6} + \cdots$$

$$- \frac{m_s^2 \langle g_s^3 fG^3 \rangle}{72\pi^2 M^8} - \frac{m}{}$$

References	m_G [MeV]
This work (BFTSR), direct Eq. (15)	$2344.60^{+213.52}_{-160.93}$
This work (BFTSR), expanded Eq. (18)	$2367.25^{+239.52}_{-167.67}$
Quenched Lattice QCD [51]	2395 ± 14
BESIII 2011 [16]	$2376.3 \pm 8.7(\text{stat}) \pm 3.3(\text{syst})$
BESIII 2020 [17]	$2341.6 \pm 8.7(\text{stat}) \pm 5.7(\text{syst})$
BESIII 2024 [18]	$2376 \pm 8.7(\text{stat})^{+26}_{-94}(\text{syst})$
BESIII 2026 [52]	2359^{+13}_{-14}

New sum rule for the R_2, which inversely fix the mass of pseudoscalar glueball

Following similar SR procedures, ρ meson longitudinal leading twist DA

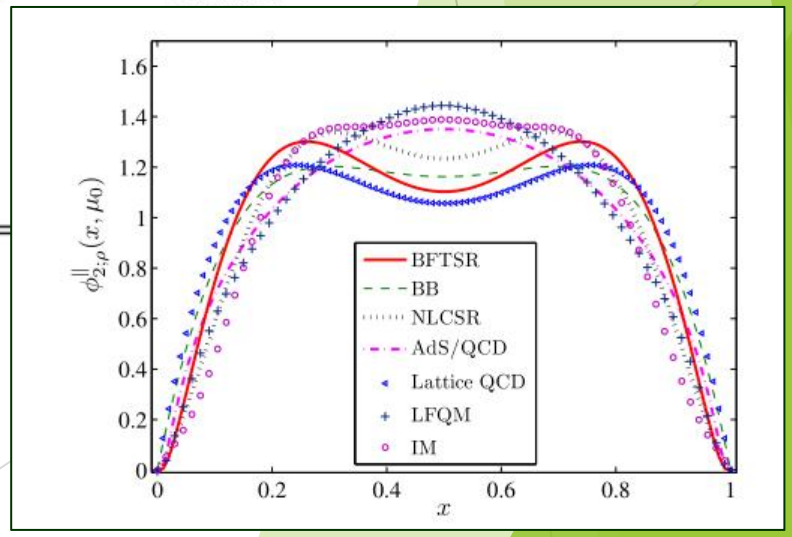
Correlator

$$\Pi_\rho^{(n,0)}(z,q) = i\int d^4x e^{iq\cdot x}\langle 0|T\{J_n(x)J_0^\dagger(0)\}|0\rangle = (z\cdot q)^{n+2} I^{(n,0)}(q^2)$$

$$J_n(x) = \bar{d}(x)\not{z}(iz\cdot \overleftrightarrow{D})^n u(x)$$

TABLE II. The first two Gegenbauer moments $a^{\parallel}_{2;\rho}$ and $a^{\parallel}_{4;\rho}$ for the longitudinal leading-twist DA $\phi^{\parallel}_{2;\rho}$, which is predicted from the sum rules under the BFT. A comparison of predictions under various approaches [9–16] has also been presented. For easy comparison, we have set the scale $\mu_0 = 1$ GeV. The moments $\langle \xi^{\parallel}_{2;\rho}\rangle$ and $\langle \xi^{\parallel}_{4;\rho}\rangle$ and the inverse moment $\langle x^{-1}\rangle$ are also presented. The number in the parentheses shows the uncertainties from all the input parameters.

	$a^{\parallel}_{2;\rho}$	$a^{\parallel}_{4;\rho}$	$\langle \xi^{\parallel}_{2;\rho}\rangle$	$\langle \xi^{\parallel}_{4;\rho}\rangle$	$\langle x^{-1}\rangle$
Our predictions	0.119(82)	−0.035(100)	0.241(28)	0.109(10)	3.30(34)
NLCSR [9]	0.047(58)	−0.057(118)	0.216(21)	0.089(9)	2.97(39)
BB [10]	0.150(70)	...	0.251(24)	...	
Lattice QCD [11]	0.197(158)	...	0.268(54)	...	
BS [12]	0.111	0.036	0.238	0.115	
AdS/QCD [13,14]	0.104	0.053	0.236	0.115	
LFQM [15]	0.014	−0.005	0.205	0.088	
IM [16]	−0.010	−0.033	0.196	0.080	



Phys. Rev. D 94, 074004 (2016)

Following similar SR procedures, ϕ meson longitudinal leading twist DA

s quark mass effect

$$
\begin{aligned}
\frac{(f_\phi^\parallel)^2\langle\xi_{2;\phi}^{\parallel;n}\rangle|_\mu\langle\xi_{2;\phi}^{\parallel;0}\rangle|_\mu}{M^2e^{m_\phi^2/M^2}} &= \frac{1}{\pi}\frac{1}{M^2}\int_{4m_s^2}^{s_\phi} ds e^{-s/M^2}\mathrm{Im}I_{2;\phi}^{\mathrm{pert}}(s) + \frac{2m_s\langle\bar{s}s\rangle}{M^4} + \frac{\langle\alpha_s G^2\rangle}{12\pi M^4}\frac{1+n\theta(n-2)}{n+1} - \frac{8n+1}{9}\frac{m_s\langle g_s\bar{s}\sigma TGs\rangle}{M^6} \\
&+ \frac{\langle g_s\bar{s}s\rangle}{81M^6}4(2n+1) - \frac{\langle g_s^3fG^3\rangle}{48\pi^2M^6}n\theta(n-2) + \frac{\sum\langle g_s^2\bar{q}q\rangle^2}{486\pi^2M^6}\left\{-2(51n+25)\left(-\ln\frac{M^2}{\mu^2}\right)\right. \\
&\left. + 3(17n+35) + \theta(n-2)\left[2n\left(-\ln\frac{M^2}{\mu^2}\right) - 25(2n+1)\tilde{\psi}(n) + \frac{1}{n}(49n^2+100n+56)\right]\right\} \\
&+ m_s^2\left\{-\frac{\langle\alpha_s G^2\rangle}{6\pi M^6}\left[\theta(n-2)(n\tilde{\psi}(n)-2) - n - 2 + 2n\left(-\ln\frac{M^2}{\mu^2}\right)\right]\right. \\
&+ \frac{\langle g_s^3fG^3\rangle}{288\pi^2M^8}\left\{-10\delta^{n0} + \theta(n-2)\left[4n(2n-1)\left(-\ln\frac{M^2}{\mu^2}\right) - 4n\tilde{\psi}(n) + 8(n^2-n+1)\right]\right. \\
&+ \theta(n-4)[2n(8n-1)\tilde{\psi}(n) - (19n^2+19n+6)] + 8n(3n-1)\left(-\ln\frac{M^2}{\mu^2}\right) - (21n^2+53n-6)\Big\} \\
&- \frac{\sum\langle g_s^2q\bar{q}\rangle^2}{972\pi^2M^8}\left\{6\delta^{n0}\left[16\left(-\ln\frac{M^2}{\mu^2}\right) - 3\right] + \theta(n-2)\left[8(n^2+12n-12)\left(-\ln\frac{M^2}{\mu^2}\right)\right.\right. \\
&- 2(29n+22)\tilde{\psi}(n) + 4\left(5n^2-2n-33+\frac{46}{n}\right)\Big] + \theta(n-4)[2(56n^2-25n+24)\tilde{\psi}(n) \\
&\times(139n^2+91n+54)] + 8(27n^2-15n-11)\left(-\ln\frac{M^2}{\mu^2}\right) - 3(63n^2+159n-50)\Big\} \\
&+ \frac{4(n-1)}{3}\frac{m_s\langle\bar{s}s\rangle}{M^6} + \frac{8n-3}{9}\frac{m_s\langle g_s\bar{s}\sigma TGs\rangle}{M^8} - \frac{4(2n+1)}{81}\frac{\langle g_s\bar{s}s\rangle^2}{M^8}\Big\},
\end{aligned}
$$

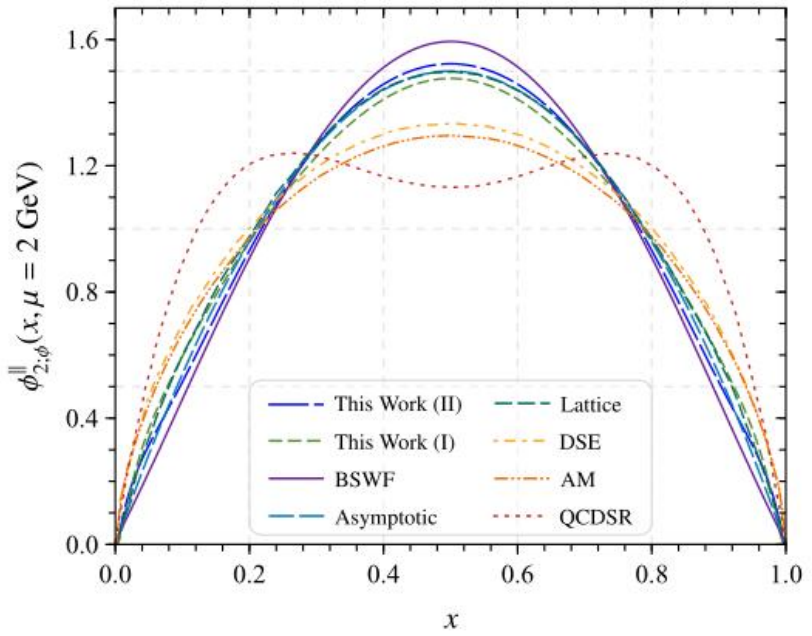


FIG. 3. Model I and II ϕ-meson longitudinal leading-twist LCDA $\phi_{2;\phi}^{\parallel}(x,\mu)$ at the scale $\mu = 2$ GeV. As a comparison, the results derived from the QCD SR [41], DSE [43], BSWF [44], AM [45], lattice QCD [46] approaches have been presented. The usual asymptotic behavior [68] for $\mu \to \infty$ is also presented.

Phys. Rev. D 110, 056017 (2024)

3. Their applications to heavy-to-light meson decays

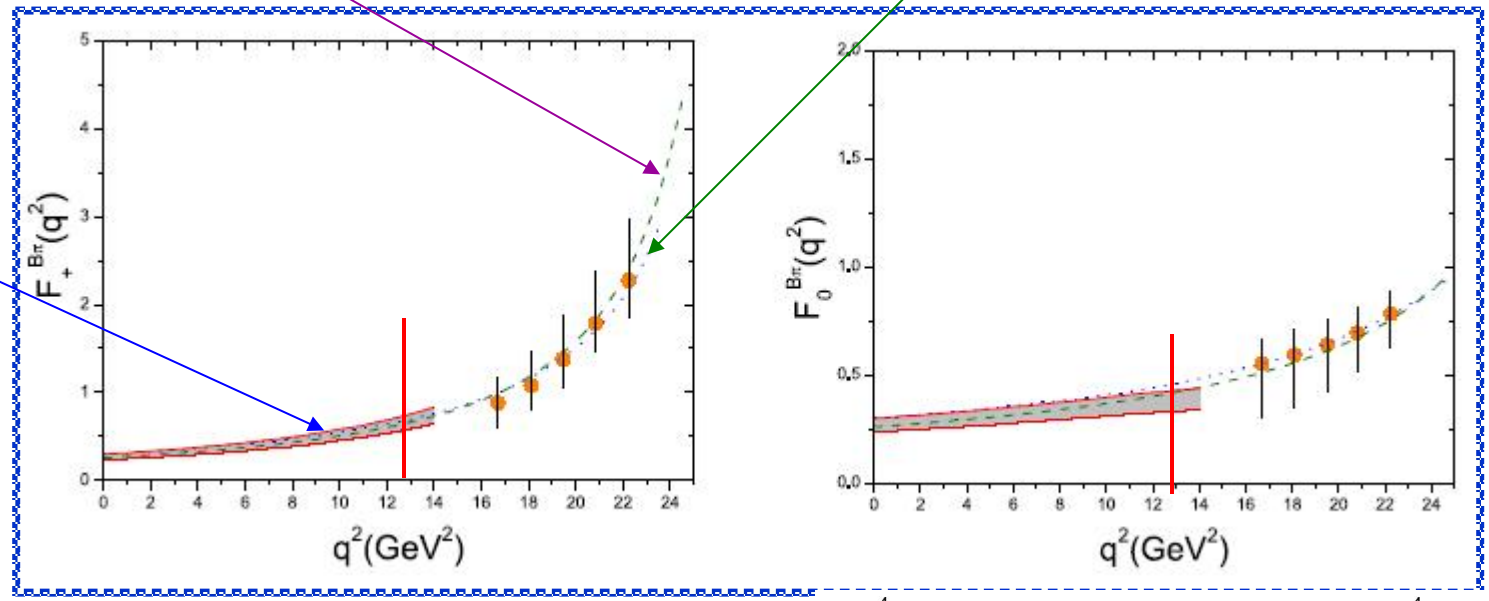
Three complementary methods
QCD sum rules as central bridge between them

QCD LCSR

LQCD

PQCD

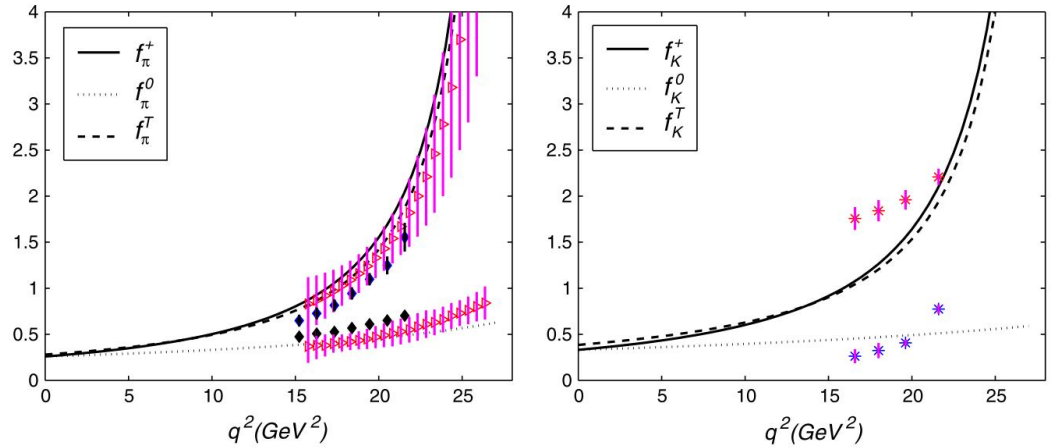
B -> π



Phys. Rev. D 71, 034018 (2005)
Phys. Rev. D 73, 074004 (2006)

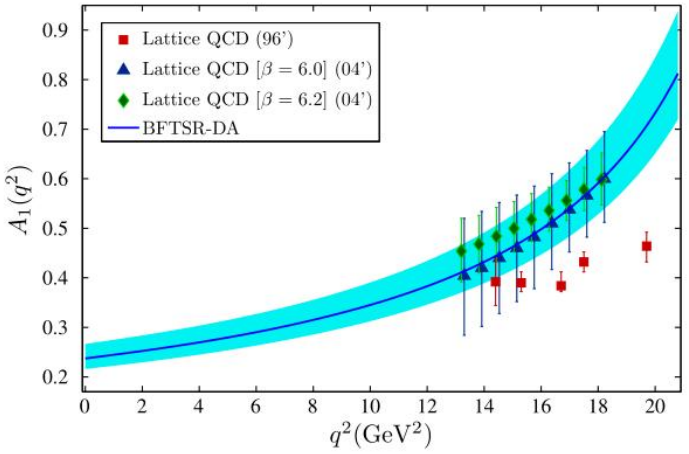
Phys. Rev. D 79, 014013 (2009)

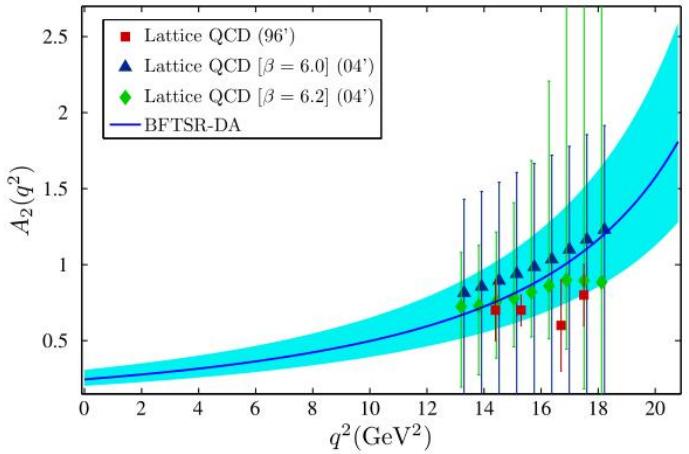
B -> K

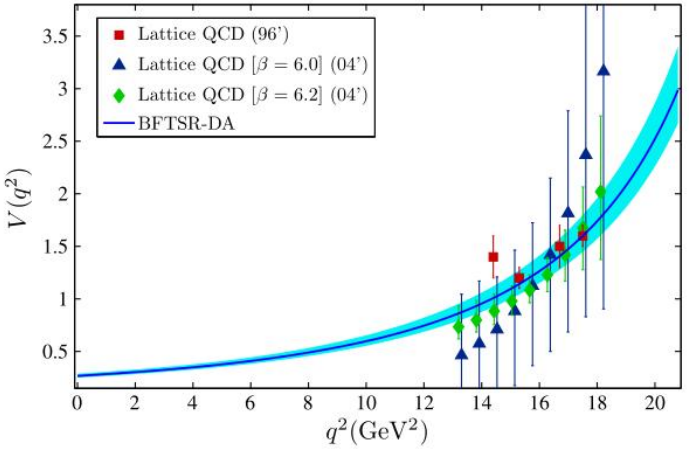


B -> ρ

Phys. Rev. D 94, 074004 (2016)







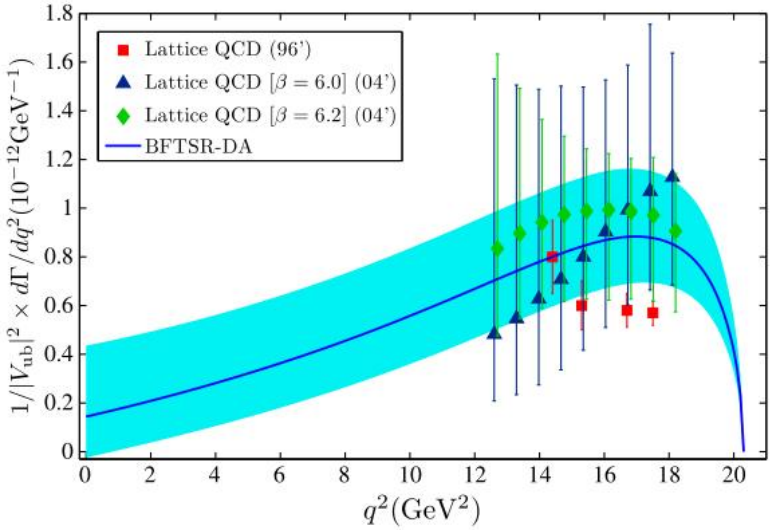
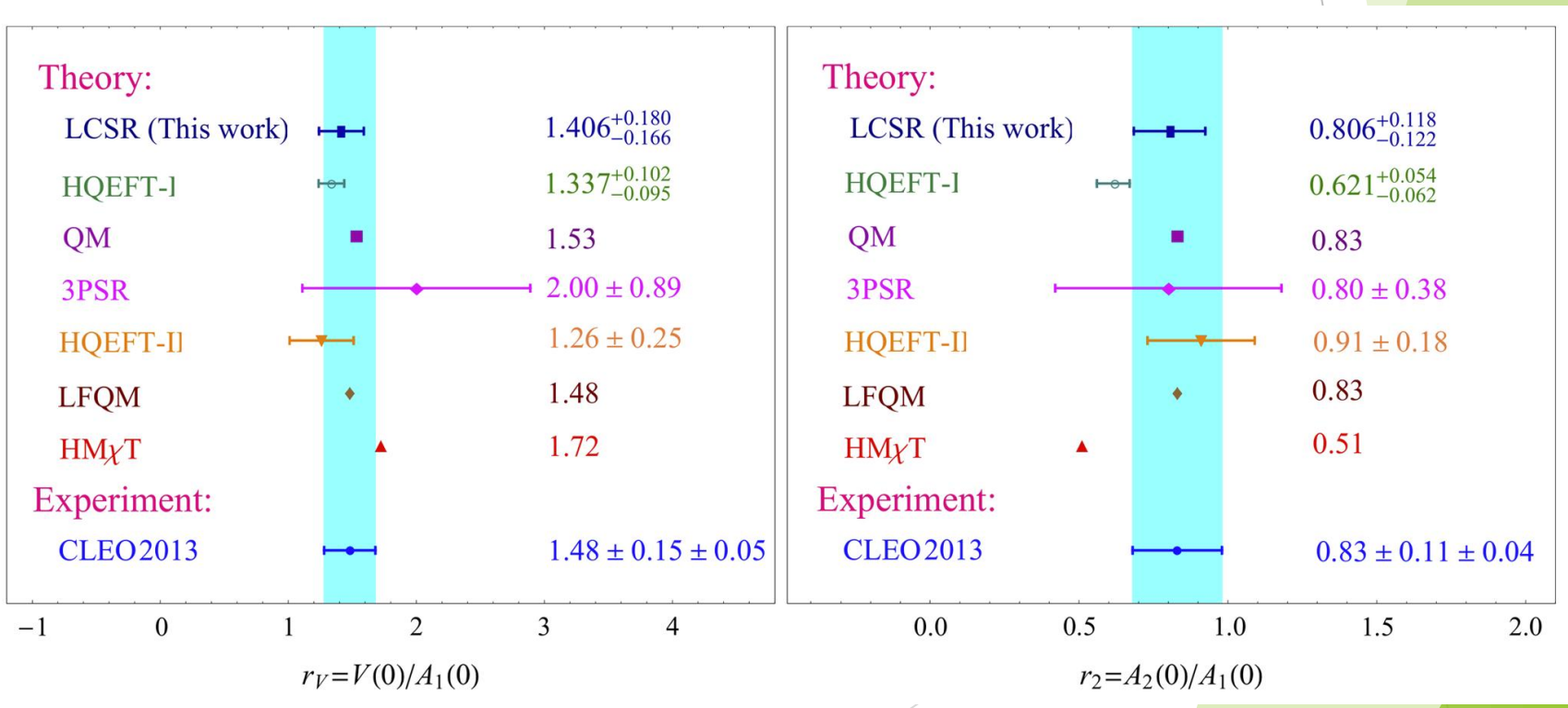


FIG. 5. The predicted differential decay width $1/|V_{ub}|^2 \times d\Gamma/dq^2$, where the shaded band shows the squared average of all the errors from the mentioned error sources. The lattice QCD predictions [65,66] are presented as a comparison.

D -> ρ

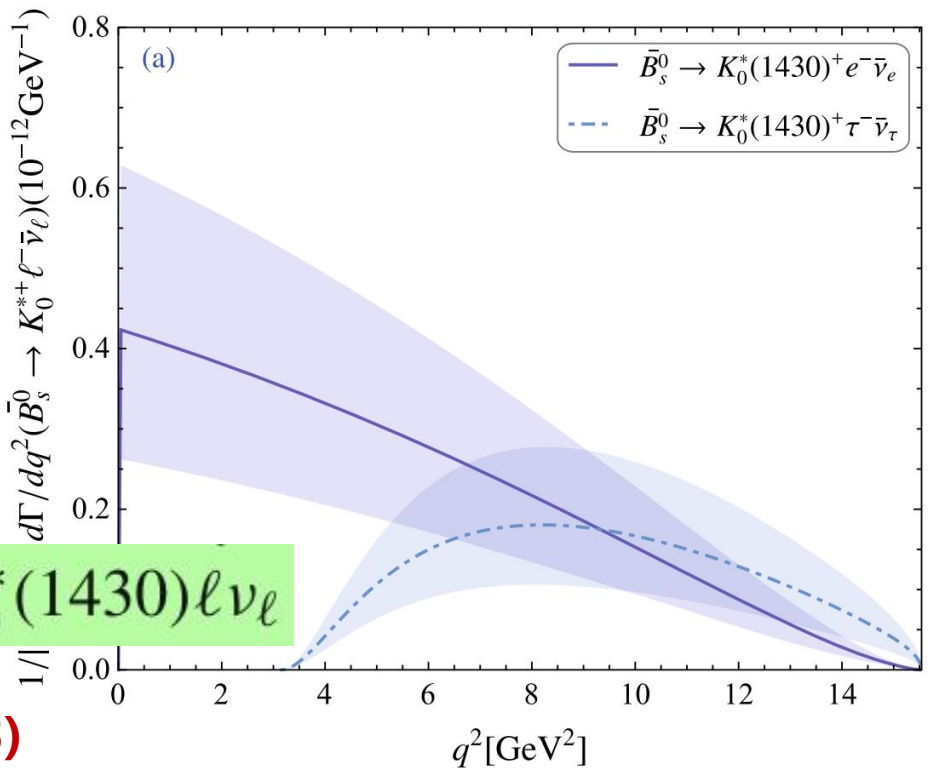
Eur.Phys.J. C80, 194 (2020)

Decay Mode	$D^0 \to \rho^- e^+ \nu_e$	$D^+ \to \rho^0 e^+ \nu_e$
This paper	$1.749^{+0.421}_{-0.297} \pm 0.006$	$2.217^{+0.534}_{-0.376} \pm 0.015$
CLEO2005 [2]	$1.94 \pm 0.39 \pm 0.13$	$2.1 \pm 0.4 \pm 0.1$
CLEO2013 [3]	$1.77 \pm 0.12 \pm 0.10$	$2.17 \pm 0.12^{+0.12}_{-0.22}$
3PSR [6]	0.5 ± 0.1	–
HQEFT [7]	1.4 ± 0.3	–
NWA [58]+HQEFT [8]	1.67 ± 0.27	2.16 ± 0.36
NWA [58]+LFQM [12]	1.73 ± 0.07	2.24 ± 0.09
FK [13]	2.0	2.5
ISGW2 [59]	1.0	1.3



decays $B_s, D_s \to K_0^*(1430)\ell\nu_\ell$

Eur.Phys.J.C 83, 7 (2023)



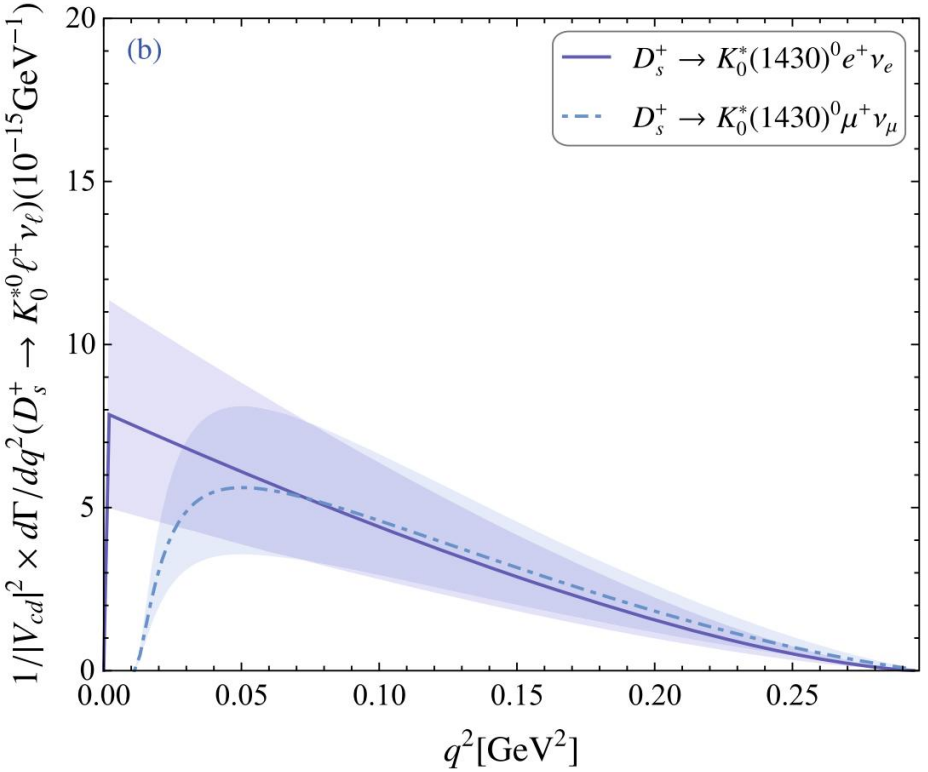
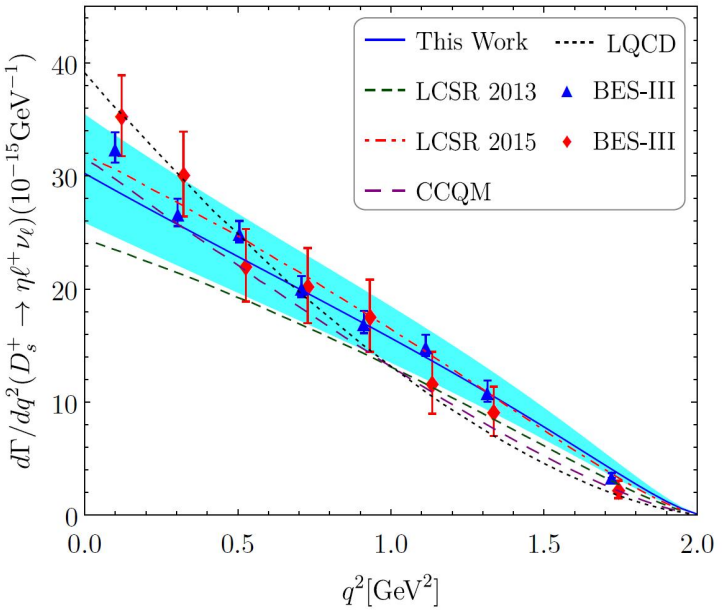


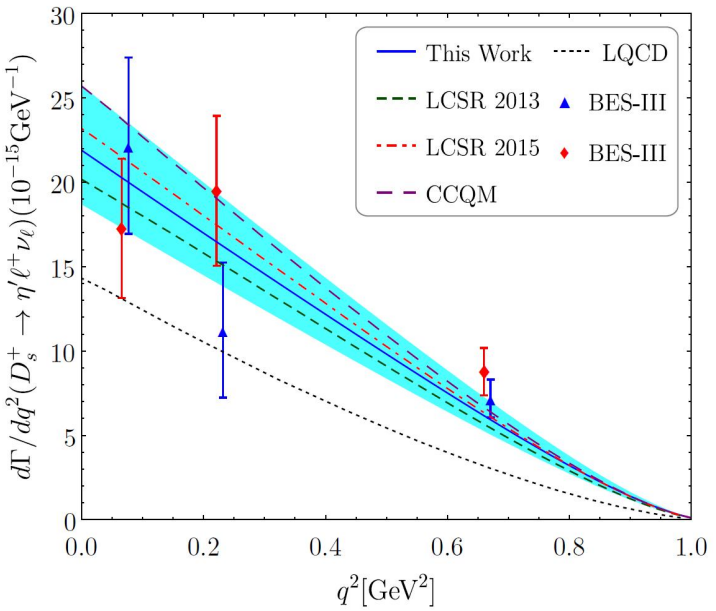
TABLE VIII: Branching fractions ($\times 10^4$) of the semileptonic decays $\overline{B}_s^0 \to K_0^*(1430)^+\ell^-\bar{\nu}_\ell$ with $\ell = e, \mu$ and τ, respectvely.

	$\mathcal{B}(\overline{B}_s^0 \to K_0^*(1430)^+ e^-\bar{\nu}_e)$	$\mathcal{B}(\overline{B}_s^0 \to K_0^*(1430)^+ \mu^-\bar{\nu}_\mu)$	$\mathcal{B}(\overline{B}_s^0 \to K_0^*(1430)^+ \tau^-\bar{\nu}_\tau)$
This work	$1.13^{+0.74}_{-0.51}$	$1.13^{+0.74}_{-0.51}$	$0.50^{+0.40}_{-0.25}$
Ref. [2]	$0.71^{+0.14}_{-0.14}$	$0.71^{+0.14}_{-0.14}$	$0.21^{+0.04}_{-0.04}$
Ref. [3]	$2.45^{+1.77}_{-1.05}$	$2.45^{+1.77}_{-1.05}$	$1.09^{+0.82}_{-0.47}$
Ref. [8](I)	–	$0.99^{+0.89}_{-0.37}$	$0.49^{+0.33}_{-0.17}$
Ref. [8](II)	–	$1.67^{+1.32}_{-0.53}$	$0.71^{+0.57}_{-0.26}$
Ref. [8](III)	–	$1.90^{+1.48}_{-0.63}$	$0.65^{+0.55}_{-0.24}$
Ref. [9]	$1.3^{+1.3}_{-0.4}$	$1.3^{+1.2}_{-0.4}$	$0.52^{+0.57}_{-0.18}$
Ref. [11]	$1.27^{+0.36}_{-0.36}$	$1.27^{+0.36}_{-0.36}$	$0.54^{+0.16}_{-0.16}$

$D_s \to \eta^{(\prime)} \ell \nu$ decays

Eur.Phys.J.C 82, 1 (2022)



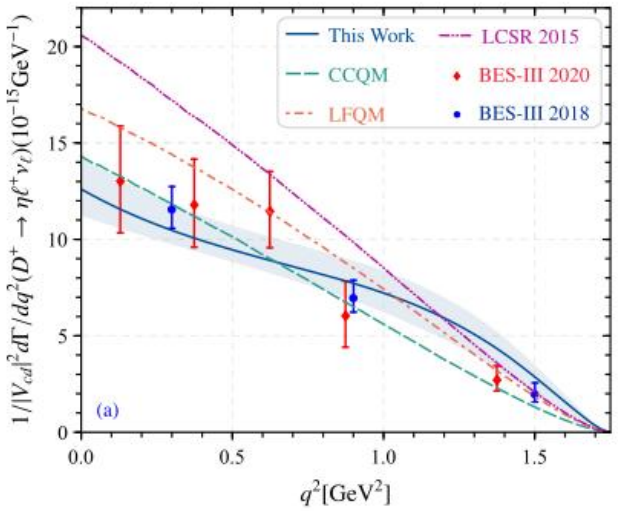


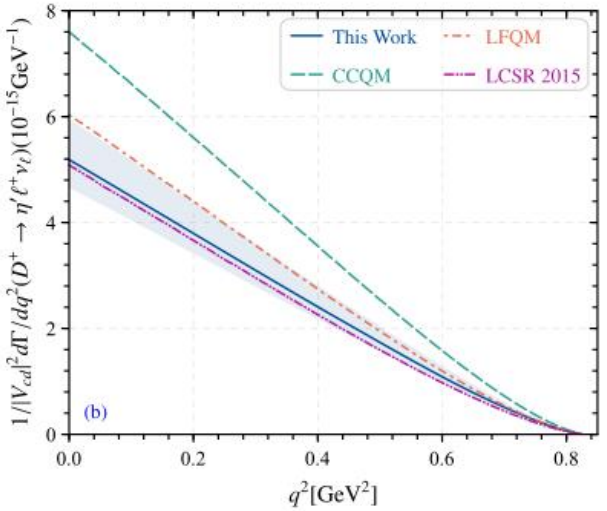
Mode	$\mathcal{B}(D_s^+ \to \eta e^+ \nu_e)$	$\mathcal{B}(D_s^+ \to \eta \mu^+ \nu_\mu)$	$\mathcal{B}(D_s^+ \to \eta' e^+ \nu_e)$	$\mathcal{B}(D_s^+ \to \eta' \mu^+ \nu_\mu)$
This work (LCSR)	$2.346^{+0.418}_{-0.331}$	$2.320^{+0.413}_{-0.327}$	$0.775^{+0.137}_{-0.114}$	$0.756^{+0.134}_{-0.111}$
BESIII [6, 7]	$2.323 \pm 0.063 \pm 0.063$	$2.42 \pm 0.46 \pm 0.11$	$0.824 \pm 0.073 \pm 0.027$	$1.06 \pm 0.54 \pm 0.07$
PDG [93]	2.32 ± 0.08	2.4 ± 0.5	0.80 ± 0.07	1.1 ± 0.5
CLEO [4]	$2.48 \pm 0.29 \pm 0.13$	-	$0.91 \pm 0.33 \pm 0.05$	-
CLEO [3]	$2.28 \pm 0.14 \pm 0.19$	-	$0.68 \pm 0.15 \pm 0.06$	-
CCQM [32]	2.24	2.18	0.83	0.79
LFQM [27]	2.26 ± 0.21	2.22 ± 0.20	0.89 ± 0.09	0.85 ± 0.08
QCD SR-I [16]	2.6 ± 0.7	-	0.89 ± 0.34	-
QCD SR-II [16]	2.3 ± 0.4	-	1.0 ± 0.2	-
LCSR [17]	2.40 ± 0.28	-	0.79 ± 0.14	-
LCSR [57]	2.00 ± 0.32	-	0.75 ± 0.23	-

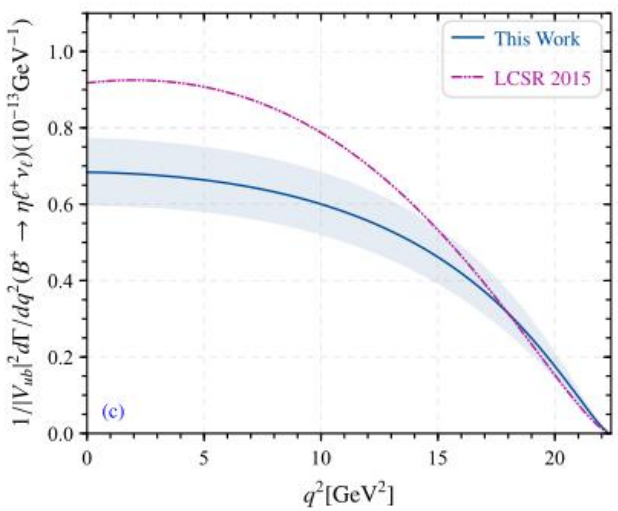
$B(D)^+ \to \eta^{(\prime)} \ell^+ \nu_\ell$ decays

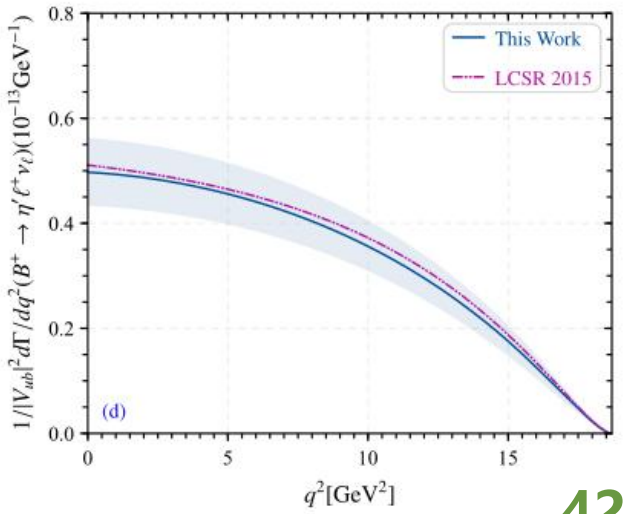
Phys. Rev. D 114, 016003 (2026)

Mode	Channels	$\lvert V_{cd}\rvert$
This work	$D^+ \to \eta e^+ \nu_e$	$0.236^{+0.017}_{-0.017}$
This work	$D^+ \to \eta \mu^+ \nu_\mu$	$0.228^{+0.017}_{-0.017}$
This work	$D^+ \to \eta' e^+ \nu_e$	$0.253^{+0.028}_{-0.032}$
BESIII 2020 [28]	$D^+ \to \eta \mu^+ \nu_\mu$	$0.242 \pm 0.028 \pm 0.033$
BESIII 2013 [16]	$D^+ \to \mu^+ \nu_\mu$	$0.221 \pm 0.006 \pm 0.005$
BaBar 2014 [17]	$D^0 \to \pi^- e^+ \nu_e$	$0.206 \pm 0.007 \pm 0.009$
CLEO 2009 [18]	$D \to \pi e^+ \nu_e$	$0.234 \pm 0.009 \pm 0.025$
HFLAV [19]	$D \to \pi \ell \nu_\ell$	$0.225 \pm 0.003 \pm 0.006$
LQCD 2019 [20]	$D \to \pi \ell \nu$	0.233 ± 0.137
PDG [24]	$D \to \pi \ell \nu$	$0.233 \pm 0.003 \pm 0.013$
	Channels	$\lvert V_{ub}\rvert \times 10^{-3}$
This work	$B^+ \to \eta \ell^+ \nu_\ell$	$3.752^{+0.373}_{-0.351}$
This work	$B^+ \to \eta' \ell^+ \nu_\ell$	$3.888^{+0.688}_{-0.787}$
CLEO 2007 [15]	$B^0 \to \pi^- \ell^+ \nu$	$3.60 \pm 0.4 \pm 0.2$
HFLAV [19]	$B \to \pi \ell \nu_\ell$	$3.70 \pm 0.10 \pm 0.12$
BaBar 2011 [21]	$\bar{B} \to X_u \ell \bar{\nu}$	$4.33 \pm 0.24 \pm 0.15$
Belle [22]	$B \to X_u \ell \nu$	$4.09 \pm 0.39 \pm 0.18$
PDG [24]	$B \to \pi \ell \bar{\nu}$	3.82 ± 0.20
PDG [24]	$B \to X_u \ell \bar{\nu}$	$4.13 \pm 0.12 \pm 0.18$
LQCD 2015 [105]	$B \to \pi \ell \nu$	3.72 ± 0.16









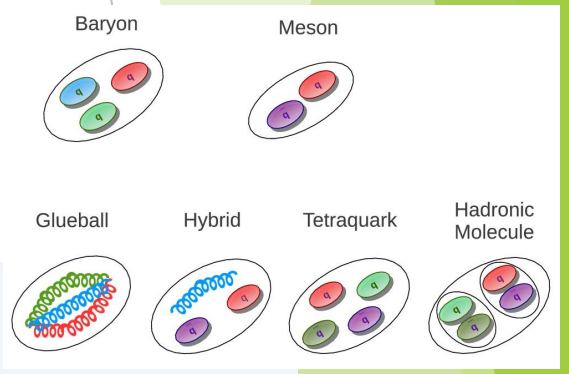
4. Summary and Outlook

PQCD+LQCD+QCDSR, 各方法均有其优缺点
方法做到极致，或各有新天地

Every method has its strengths and limitations

— pushing further may open new horizons

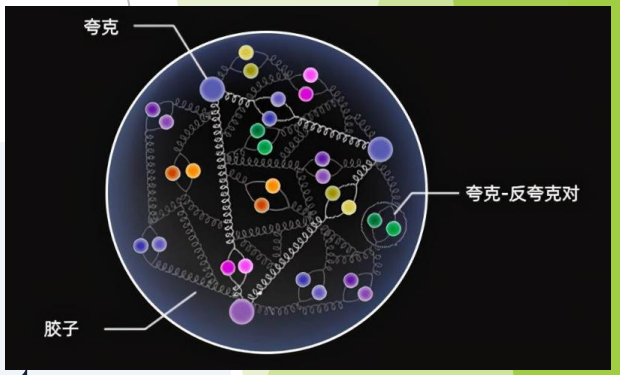
QCD求和规则：优势、局限与展望
QCD Sum Rules: Strengths, Limitations, and Outlook



Role and Scope

- QCD sum rules can play an important role and can be extended to **broader scenarios**, such as **exotic hadron states** (tetraquarks, pentaquarks, glueballs, hybrids)
- QCD sum rules are **approximate relations** — they rely on OPE truncation, Borel-window stability, and continuum modeling. Yet they are empirically helpful and deserve continued study: they provide **a systematic analytic access to non-perturbative hadron structure**, and their uncertainties are under control and quantifiable

QCD求和规则：优势、局限与展望
QCD Sum Rules: Strengths, Limitations, and Outlook



Possible directions for improvement (methodological improvements)

- Adopt double **Borel transformation** or new way for enhanced stability
- Systematically analyze ground-state, continuum, and excited-state contributions
  - ✓ Improve the precision of the **model parameters**
  - ✓ Include **higher-dimensional** operator contributions
  - ✓ Incorporate **higher-twist** distribution amplitude contributions
  - ✓ Compute **higher-order** perturbative corrections
- How to generalize **beyond the valence-quark model** to complex scenarios ?
- How to suppress or effective **estimate unknown contributions** reliably / precisely ?

AI will have some help to improve the precision of SR predictions